*Geochimica et Cosmochimica Acta* Vol. 57, pp. 795–814
1993 Pergamon Press Ltd. Printed in U.S.A.

0016-7037/93/$6.00 + .00

# Oxygen buffering of Kilauea volcanic gases and the oxygen fugacity of Kilauea basalt

T. M. GERLACH
US Geological Survey, Cascades Volcano Observatory, 5400 MacArthur Blvd., Vancouver WA 98661, USA

(*Received February* 25, 1992; *accepted in revised form August* 6, 1992)

**Abstract**—Volcanic gases collected during episode 1 of the Puu Oo eruption along the east rift zone of Kilauea Volcano, Hawaii, have uniform C-O-H-S-Cl-F compositions that are sharply depleted in $CO_2$. The $CO_2$-poor gases are typical of Type II volcanic gases (GERLACH and GRAEBER, 1985) and were emitted from evolved magma stored for a prolonged period of time in the east rift zone after releasing $CO_2$-rich gases during an earlier period of temporary residence in the summit magma chamber. The samples are remarkably free of contamination by atmospheric gases and meteoric water. Thermodynamic evaluation of the analytical data shows that the episode 1 gases have equilibrium compositions appropriate for temperatures between 935 and 1032°C. Open- and closed-system equilibrium models of species distributions for the episode 1 gases show unequivocally that coexisting lavas buffered the gas oxygen fugacities during cooling. These models indicate that the $f_{O_2}$ buffering process occurs by transfer of oxygen from the major species in the gas phase ($H_2O$, $CO_2$, $SO_2$) to the lava during cooling and that the transfer of oxygen also controls the fugacities of several minor and trace species ($H_2$, CO, $H_2S$, $S_2$, $Cl_2$, $F_2$), in addition to $O_2$ during cooling. Gas/lava exchanges of other components are apparently insignificant and exert little influence, compared to oxygen exchange, during cooling. Oxygen transfer during cooling is variable, presumably reflecting short-term fluctuations in gas flow rates. Higher flow rates restrict the time available for gas/lava oxygen transfer and result in gases with higher equilibrium temperatures. Lower flow rates favor $f_{O_2}$-constrained equilibration by oxygen transfer down to lower temperatures. Thus, the chemical equilibrium preserved in these gases is a heterogeneous equilibrium constrained by oxygen fugacity, and the equilibrium temperatures implied by the compositions of the gases reflect the temperatures at which gas/lava oxygen exchange ceased. This conclusion challenges the common assumption that volcanic gases are released from lava in a state of chemical equilibrium and then continue equilibrating homogeneously with falling temperature until reaction rates are unable to keep pace with cooling. No evidence is found, moreover, that certain gas species are kinetically more responsive and able to equilibrate down to lower temperatures than those of the last gas/lava oxygen exchange. Homogeneous reaction rates in the gas phase are apparently slow compared to the time it took for the gases to move from the last site of gas/lava equilibration to the site of collection. An earlier set of data for higher temperature $CO_2$-rich Type I volcanic gases, which come from sustained summit lava lake eruptions supplied by magma that experienced substantially shorter periods of crustal storage, shows $f_{O_2}$ buffering by oxygen transfer up to 1185°C. Oxygen fugacity measurements in drill holes into ponded lava flows suggest that buffering by oxygen transfer may control the $f_{O_2}$ of residual gases down to several hundred degrees below the solidus in the early stages of cooling. Although the details of the $f_{O_2}$ buffering mechanisms for oxygen transfer are unknown, the fact that $f_{O_2}$ buffering is effective from molten to subsolidus conditions suggests that the reaction mechanisms must change with cooling as the reactants change from predominantly melt, to melt plus crystals, to glass plus crystals. Mass balance calculations suggest that redox reactions between the gas and ferrous/ferric iron in the lava are plausible mechanisms for the oxygen transfer and that the $f_{O_2}$ of the gases is buffered by sliding ferrous/ferric equilibria in the erupting lavas. Contrary to expectations based on models predicting the oxidation of basalt by $H_2$ and CO escape during crustal storage, $CO_2$-rich Type I gases and $CO_2$-poor Type II gases have identical oxygen fugacities despite greatly different crustal storage and degassing histories. Volcanic gas data give a tightly constrained log $f_{O_2}$ of NNO − 0.5 (±0.05) for subaerially erupted Kilauea basalt from liquidus to solidus temperatures, consistent with recent $f_{O_2}$ determinations for the mantle source regions of ocean island basalts. Because the oxygen fugacities of volcanic gases emitted by subaerial lavas imply that the $f_{O_2}$ of Kilauea basalt is unchanged during crustal storage, Kilauea basalt either arrives in the crust with an oxygen fugacity between NNO and FMQ, or it develops an oxygen fugacity in this range immediately upon arrival in the summit chamber.

## INTRODUCTION

KILAUEA VOLCANO IS LOCATED adjacent to the southeastern flank of Mauna Loa Volcano (Fig. 1). Its southern flank is detached from the stable shield to the north by the east and southwest rift zones (SWANSON et al., 1976). The summit and the east rift zone (ERZ) are the most active eruption and intrusion sites. Geodetic and seismic data indicate the presence of a magma chamber in the form of a dike and sill complex beneath the summit (FISKE and KINOSHITA, 1969; RYAN et al., 1981). The roof and base of the chamber lie approximately 2 km and 6 km, respectively, under the summit caldera floor (RYAN et al., 1981). Mantle sources at 30–

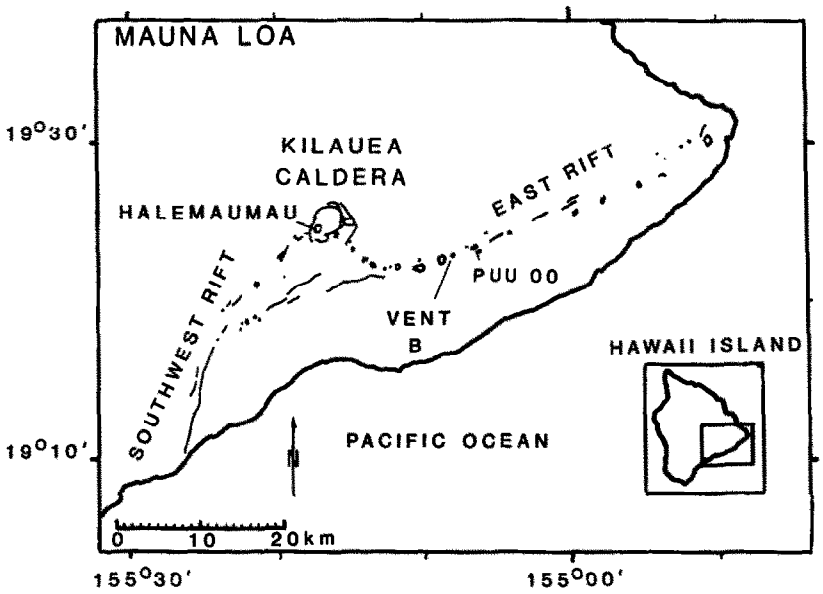


FIG. 1. Map of the summit caldera, the southwest rift zone, and the east rift zone (ERZ) of Kilauea Volcano, Hawaii. The ERZ continues along its subaerial northeast trend for about 70 km under the sea. The Puu Oo eruption began 3 January 1983 about 2 km southwest of Vent B and extended several kilometers along fissures to the northeast. It subsequently became centered at Puu Oo vent. The gas samples for this study came from a vigorously fuming fissure at Vent B.

90 km depth feed magma through a conduit to the summit chamber (ELLSWORTH and KOYANAGI, 1977; RYAN et al., 1981) at a long-term average rate of about 0.1 $km^3$/yr (DZURISIN et al., 1984). Throughout most of this century, the magma supplied from the mantle has remained temporarily in the summit chamber before being injected into the rift zones, where geodetic, petrologic, and magma budget data indicate substantial quantities of magma have accumulated (WRIGHT and FISKE, 1971; SWANSON et al., 1976; DZURISIN et al., 1984). Occasionally, however, the top of the chamber has risen into Halemaumau pit crater (Fig. 1) and produced continuously supplied lava lake eruptions on the floor of the summit caldera (MACDONALD and ABBOTT, 1970).

Volatile degassing from Kilauea Volcano occurs in two ways. When magma ascends continuously to the surface to sustain summit lava lake eruptions at Halemaumau, relatively $CO_2$-rich volcanic gases, the Type I gases of GERLACH and GRAEBER (1985), are emitted in a one-stage degassing process (Fig. 2a; Table 1). A more complex two-stage degassing process occurs when magma injected into the summit chamber remains there long enough to equilibrate to chamber conditions (Fig. 2b). The first stage consists of the quiescent degassing of $CO_2$, $SO_2$, and $H_2O$ in excess of melt solubilities from the summit chamber in a chamber gas that is more $CO_2$-rich than the Type I volcanic gases and estimated to contain up to 80 mol% $CO_2$ (GERLACH and GRAEBER, 1985). The second stage of degassing is the emission of $CO_2$-poor volcanic gases (<10 mol% $CO_2$), the Type II gases of GERLACH and GRAEBER (1985), during subaerial eruptions of reservoir-equilibrated magma (Fig. 2b). Most eruptions of Kilauea Volcano in this century involved magma in the second stage of the two-stage degassing process (GERLACH and GRAEBER, 1985).

In this study, I use volcanic gas data to investigate the oxygen fugacity of Kilauea basalt from liquidus to subsolidus conditions. The study has the following objectives:

1) To report chemical data for Type II volcanic gas samples collected in mid-January 1983 during episode 1 of the Puu Oo eruption on the ERZ and to evaluate the data for the effects of contamination and sampling errors;
2) to show that episode 1 lavas buffered the oxygen fugacities of the Type II volcanic gas emissions and that Kilauea lavas similarly buffer the oxygen fugacities of Type I volcanic gas emissions from summit lava lakes and of residual gas emissions from ponded lava flows;
3) to show that oxygen fugacity buffering of volcanic gases by Kilauea lavas also controls the fugacities of other minor and trace species in the gas phase;
4) to demonstrate that the oxygen fugacity buffering is consistent with mechanisms that transfer oxygen from the gas to the lava during cooling;
5) to illustrate that the state of chemical equilibrium preserved in Kilauea volcanic gases is an equilibrium constrained by lava oxygen fugacity buffering and indicative of the conditions when gas/lava oxygen exchange ceased;
6) to derive an equation based on volcanic gas data for the oxygen fugacity of subaerial Kilauea basalt from liquidus to subsolidus temperatures;
7) to derive an empirical geobarometer for calculating the oxygen fugacity of Kilauea basalt directly from glass MgO content; and
8) to examine hypotheses that invoke degassing processes during mantle ascent and crustal storage (e.g., SATO, 1978; MATHEZ, 1984) for controlling the redox state of basaltic magmas, in contrast to the view that the oxygen fugacities

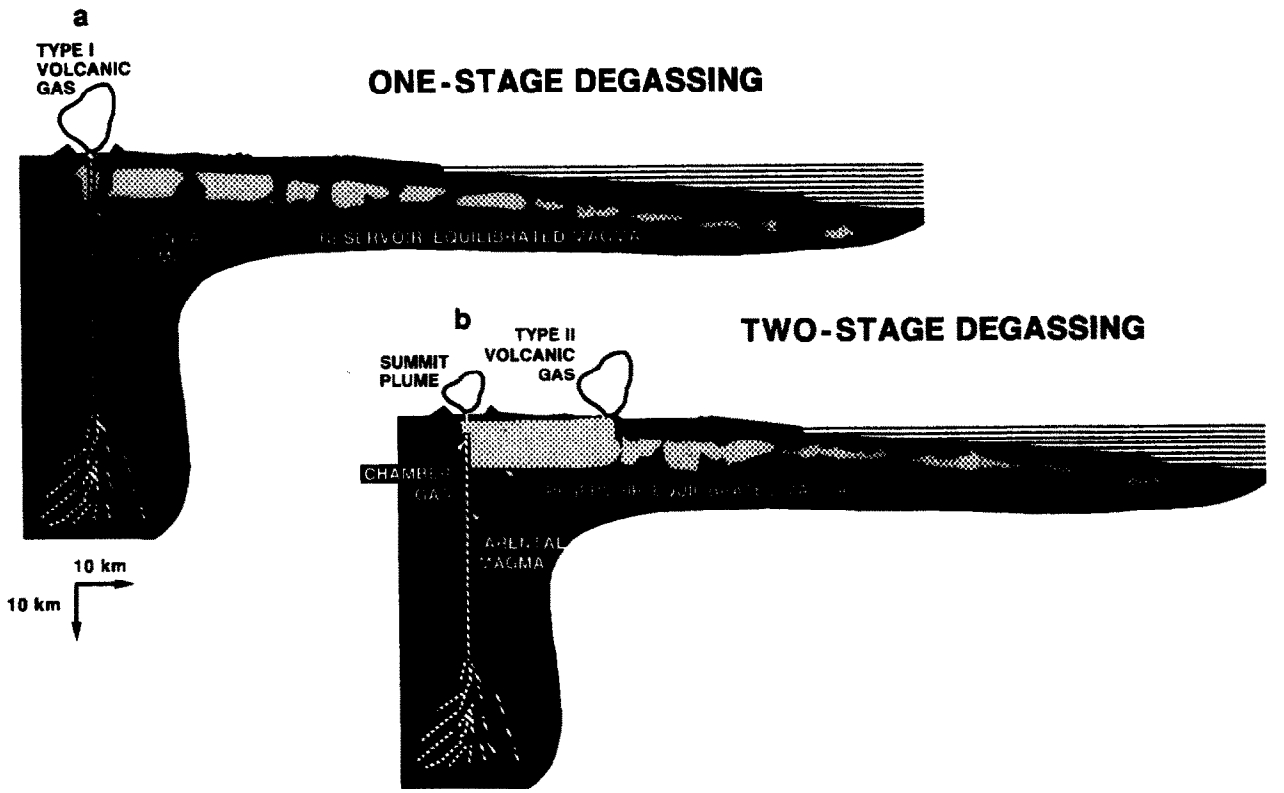


FIG. 2. Schematic cross sections, without vertical exaggeration, of the magma supply, storage, and transport system of Kilauea Volcano. The cross sections are adapted from the models of several investigators referred to in the introductory text. Each cross section begins west of the caldera and runs through Halemaumau pit crater, southeast along the upper ERZ, and east and northeast along the middle and lower ERZ (Fig. 1). The cross sections continue along the submarine ERZ out approximately 70 km to the Hawaiian Deep. For purposes of illustration, the thickness of the feeder conduit system for the parental magma supply is greatly exaggerated, and the summit magma chamber is slightly enlarged. A plexus of dikes, sheets, and conduits is believed to constitute the summit chamber and ERZ storage reservoirs shown schematically as regions with high melt-to-rock ratios. (a) A one-stage degassing process during a continuously supplied summit lava lake eruption emitting Type I volcanic gases (Table 1). (b) A two-stage degassing process involving $CO_2$-rich chamber gas venting from magma in the summit chamber and an ERZ eruption emitting $CO_2$-depleted Type II volcanic gases derived from reservoir-equilibrated magma. Minor degassing of reservoir-equilibrated magma may occur during crystallization or decompression in the rift zone reservoir complex after summit chamber gas venting and prior to eruptive emission of the Type II gases. The chamber gas supplies volatiles to the summit hydrothermal system and to the summit fumaroles and plume. Eruptions of reservoir-equilibrated magma occur in the summit region and along the rift zone at both subaerial (as shown) and submarine sites.

of basaltic magmas reflect the oxygen fugacity of their mantle source regions (CARMICHAEL, 1991).

## EPISODE 1 VOLCANIC GASES

### Geological Setting

The Puu Oo eruption began on January 3, 1983, in the middle portion of the ERZ and has continued until the time of this writing in July 1992. The results of comprehensive geologic, geophysical, geochemical, and petrologic monitoring studies are described in WOLFE (1988) for eruptive episodes 1 through 20 (3 January 1983 through 8 June 1984). The volcanic gas samples of this study are from episode 1, which was characterized by intermittent eruptive activity totaling about 100 h over the period from 3 to 23 January 1983. Fissure eruptions dominated during episode 1, and linear fountains from tens to several hundreds meters length erupted along the ERZ. The initial outbreak involved numerous vents on a fissure system that for a time occupied 8 km of the ERZ. After the fissure eruptions of episode 1, centralized vent eruptions dominated and ultimately localized at Puu Oo vent (Fig. 1) starting with episode 4 on 13 June 1983.

Episode 1 lavas originated from several isolated and evolved pockets of magma that had cooled and differentiated by crystallization to varying degrees during prolonged storage within the ERZ (GARCIA and WOLFE, 1988). The low MgO content (<6.8 wt%), depletion of CaO, and enrichment of $FeO_t$ in the episode 1 lavas indicate fractionation of clinopyroxene and plagioclase as well as olivine. Partly resorbed xenocrysts and reversely zoned phenocrysts are present, indicating magma mixing and the formation of hybrid magmas. Trace-element data also suggest the episode 1 lavas are comprised of hybrid magmas.

Thermocouple measurements in the melt of pahoehoe lava during episode 1 gave temperatures of up to 1125°C (NEAL et al., 1988). Geothermometer determinations, based on the method of HELZ and THORNBER (1987) and applied to the MgO contents of episode 1 glasses, indicate lava temperatures of up to 1145°C (R. Helz, pers. commun., April 1991).

*Collection site*

Gas samples were collected at Vent B (Fig. 1) on 14, 15, and 16 January 1983. Vent B was about 2 km northeast of Napau Crater, where the lava first surfaced on 3 January, and about 4 km southwest of Puu Oo where the eruption eventually became centered (Fig. 1).

Table 1. Type I volcanic gases based on restored compositions of 1918-19 summit lava lake gases[a]

| Sample | J-8 | J-11 | J-13 | J-14 | J-16 | J-17 | J-18 |
|---|---|---|---|---|---|---|---|
| $H_2O$ (mol %) | 37.09 | 40.14 | 69.29 | 35.09 | 60.42 | 65.95 | 58.14 |
| $H_2$ (mol %) | 0.49 | 0.55 | 1.01 | 0.54 | 0.87 | 1.02 | 1.03 |
| $CO_2$ (mol %) | 48.90 | 36.69 | 17.82 | 47.41 | 23.21 | 20.27 | 21.76 |
| CO (mol %) | 1.51 | 1.03 | 0.62 | 1.52 | 0.74 | 0.62 | 0.93 |
| $SO_2$ (mol %) | 11.84 | 21.06 | 10.93 | 15.06 | 14.31 | 11.44 | 17.46 |
| $H_2S$ (mol %) | 0.04 | 0.20 | 0.08 | 0.15 | 0.14 | 0.32 | 0.17 |
| $S_2$ (mol %) | 0.02 | 0.25 | 0.03 | 0.17 | 0.07 | 0.16 | 0.13 |
| HCl (mol %) | 0.08 | 0.00 | 0.21 | 0.00 | 0.21 | 0.17 | 0.32 |
| log $f(O_2)$ | -8.38 | -9.33 | -8.40 | -9.30 | -8.84 | -9.65 | -8.45 |
| log $f(S_2)$ | -3.70 | -2.60 | -3.52 | -2.77 | -3.15 | -2.80 | -2.89 |
| Equilibrium T (°C) | 1170 | 1100 | 1175 | 1100 | 1140 | 1085 | 1185 |

[a]From Gerlach (1980)

Magma discharged from Vent B at the start of the eruption on 3 January. Activity decreased at the vent as erupting fissures migrated northeast during the first few weeks of the eruption. Lava continued to be observed in the vicinity of Vent B just beneath the surface along fissures until 21 January 1983, and it occasionally erupted with weak fountaining.

The gas collection site at Vent B was a vigorously fuming fissure several meters long and less than a meter across at ground level. Spatter deposits and fragmented lava bridged the fissure over most of its length. Although the fissure was closed to the atmosphere at most points, a few small openings permitted access down steep fractures penetrating to incandescent lava at about 1–2 m depth.

## Sample Collection, Analysis, and Interpretation

The Appendix contains a detailed presentation of sample collection, analysis, and interpretation of results. This section summarizes only the information from the Appendix essential to the discussion that follows. All claims made here are supported fully in the fine print of the Appendix.

Temperatures were measured at Vent B before and after collection each day. They fluctuated at these times, and probably during collection as well. Average temperatures at the base of the collection tube on 14, 15, and 16 January were 935, 915, and 895°C, respectively. Ten gas samples were obtained by conventional collection procedures based on the use of evacuated bottles containing NaOH solution (GIGGENBACH, 1975). A variety of analytical techniques were applied to determine the amounts of gas species that dissolved in the NaOH solutions and accumulated in the evacuated bottle head spaces. The analytical results show that the proportion of atmospheric gases contaminating the samples is remarkably low; the total of $N_2$ + Ar + $O_2$ is generally <0.05 mol%. There is little or no evidence in the analytical data of oxidation by reaction of the reduced gases ($H_2$, CO, $H_2S$) with atmospheric $O_2$; nor is there any evidence that the samples became chemically altered by reaction with the collection equipment.

The analyses of six of the samples correspond to chemical equilibrium compositions at temperatures up to 117°C above their respective collection temperatures. Four samples deviate slightly to moderately from equilibrium compositions due mainly to sampling errors that mainly affected their water contents. Because the disequilibrium in these four samples is moderate and limited to water alterations, it is a simple matter to correct the analytical data and to show that these samples were initially equilibrium gas compositions at temperatures up to 84°C above their collection temperatures, as illustrated in the Appendix. In addition, compatible equilibrium amounts of minor and trace species ($S_2$, COS, $Cl_2$, $F_2$) that are normally not determined analytically were calculated for all the samples.

The best estimates of the episode 1 gas compositions are presented as "restored analyses" in Table 2. Table 2 contains molar abundances and mol% concentrations of major and minor species, and molar abundances of elemental components of the restored analyses. The molar abundances of species are reported to the number of significant figures warranted by the precision of the analytical data; mol% concentrations were calculated from the molar abundances and rounded to the number of significant figures. The molar abundances of elemental C, O, H, S, Cl, and F reported in Table 2 were calculated from the molar abundances of the molecular species. Included in Table 2 are the log values for the fugacities of $O_2$, $Cl_2$, and $F_2$ calculated from the restored compositions at the equilibrium temperatures. (All fugacity values in the text, figures, tables, and equations are in units of bars.) The equilibrium temperatures given in Table 2 are the temperatures implied by reaction equilibria among species in the gas phase. The results reinforce several earlier studies (e.g., MATSUO, 1961) indicating that the equilibrium temperatures implied by volcanic gas compositions tend to be higher than the vent temperatures of the collection sites.

The restored episode 1 gas compositions are poor in $CO_2$ and represent Type II volcanic gases. They are similar in their concentrations of the major species $H_2O$, $CO_2$, and $SO_2$. As a result, their elemental compositions form a tight grouping when plotted in a C-H-S ternary diagram (Fig. 3). The variations that do exist in the minor species are due mainly to the different equilibrium temperatures of the samples and to the effects of oxygen fugacity buffering, as discussed below.

### *Comparison with type I gases*

Sustained summit lava lakes existed in Halemaumau pit crater (Fig. 1) during most of the previous century and on into the early 1920s (MACDONALD and ABBOTT, 1970). They were present again during summit eruptions in 1952 and 1967–1968, but for briefer periods lasting only several months. Resupply by ascending summit magma sustained the lava lake activity at these times. In essence, the roof of the summit magma chamber rose into the pit crater to produce a continuously supplied lava lake eruption. During the previous century, sustained summit lava lake eruptions overflowed Halemaumau pit crater on occasion, often including large areas of Kilauea's caldera floor. Sustained summit lava lakes emit Type I volcanic gases (Fig. 2a), which represent degassing from the summit magma chamber at times when its roof breaks through to the surface (GERLACH and GRAEBER, 1985). The Type I gas samples (Table 1) plotted in Fig. 3 include $CO_2$-rich gases like J-8, which was collected from a crack in a spatter cone adjacent to a summit lava lake source, and gases poorer in $CO_2$ that were emitted by partially degassed lavas at the margins of a summit lava lake (GERLACH, 1980; GERLACH and GRAEBER, 1985).

Type II volcanic gases, such as the restored episode 1 compositions (Table 2), are depleted in $CO_2$ compared to Type I volcanic gases (Fig. 3). Lavas that emit Type II gases develop by degassing of a summit chamber gas more $CO_2$-rich than J-8 during the first stage of degassing from magma injected into and temporarily stored within the summit chamber before being discharged to the rift zone reservoir complex (Fig. 2b). These lavas may experience further minor degassing related to crystallization and decompression during storage and/or transport in the rift zone reservoir complex after summit chamber gas venting and prior to the eruptive emission of Type II

Table 2. Restored volcanic gas compositions for episode-1, east rift zone eruption, Kilauea Volcano, January 1983

| Sample | Pele 9 | Pele 4 | Pele 6 | Pele 12 | Pele 2 | Pele 3 | Pele 5 | Pele 7 | Pele 8 | Pele 10 |
|---|---|---|---|---|---|---|---|---|---|---|
| Date | Jan 14 | Jan 14 | Jan 14 | Jan 15 | Jan 15 | Jan 15 | Jan 15 | Jan 15 | Jan 16 | Jan 16 |
| Collection T (°C) | 935 | 935 | 935 | 915 | 915 | 915 | 915 | 915 | 895 | 895 |
| Equilibrium T (°C) | 1010 | 997 | 1016 | 935 | 948 | 952 | 1003 | 1032 | 979 | 980 |
| $H_2O$ (molx$10^4$) | 1201. | 2510. | 2139. | 2480. | 2380. | 2720. | 2390. | 2830. | 2140. | 2620. |
| $H_2$ (molx$10^4$) | 13.59 | 30.54 | 28.33 | 33.55 | 28.10 | 28.42 | 27.14 | 32.70 | 24.32 | 27.42 |
| $CO_2$ (molx$10^4$) | 47.5 | 117. | 94.8 | 99.8 | 118. | 127. | 103. | 124. | 94.1 | 99.8 |
| CO (molx$10^4$) | 0.892 | 2.16 | 2.15 | 1.84 | 1.80 | 2.08 | 1.88 | 2.76 | 1.65 | 1.65 |
| $SO_2$ (molx$10^4$) | 224. | 370. | 367. | 363. | 407. | 420. | 342. | 493. | 483. | 519. |
| $H_2S$ (molx$10^4$) | 9.36 | 23.4 | 23.4 | 101. | 51.5 | 44.6 | 17. | 18. | 34.3 | 30. |
| $S_2$ (molx$10^4$) | 4.65 | 11.0 | 11.9 | 59.6 | 33.9 | 18.2 | 6.72 | 6.92 | 22.7 | 15.6 |
| COS (molx$10^4$) | 0.0198 | 0.0505 | 0.0577 | 0.169 | 0.0967 | 0.109 | 0.0371 | 0.0523 | 0.0738 | 0.0583 |
| HCl (molx$10^4$) | 2. | 5.27 | 4.09 | 5.27 | 4.48 | 5.47 | 4.37 | 6.12 | 4.74 | 5.78 |
| HF (molx$10^4$) | 2.8 | 6.3 | 3.3 | 6.3 | 5.8 | 5.8 | 4.2 | 6.8 | 5.1 | 5.8 |
| C (molx$10^4$) | 48.4118 | 119.2105 | 97.0077 | 101.8090 | 119.8967 | 129.1890 | 104.9171 | 126.8123 | 95.8238 | 101.5083 |
| O (molx$10^4$) | 1744.9118 | 3486.2105 | 3064.8077 | 3407.6090 | 3431.8967 | 3816.1890 | 3281.9170 | 4066.8123 | 3295.9238 | 3859.3083 |
| H (molx$10^4$) | 2452.70 | 5139.45 | 4388.85 | 5240.67 | 4929.48 | 5597.31 | 4876.85 | 5774.32 | 4407.08 | 5366.42 |
| S (molx$10^4$) | 242.6798 | 415.4505 | 414.2577 | 583.3690 | 526.3967 | 501.1090 | 372.4771 | 524.8923 | 562.7738 | 580.2583 |
| Cl (molx$10^4$) | 2. | 5.27 | 4.09 | 5.27 | 4.48 | 5.47 | 4.37 | 6.12 | 4.74 | 5.78 |
| F (molx$10^4$) | 2.8 | 6.3 | 3.3 | 6.3 | 5.8 | 5.8 | 4.2 | 6.8 | 5.1 | 5.8 |
| $H_2O$ (mol %) | 79.8 | 81.6 | 80.0 | 78.7 | 78.5 | 80.7 | 82.5 | 80.4 | 76.2 | 78.8 |
| $H_2$ (mol %) | 0.9025 | 0.9929 | 1.059 | 1.065 | 0.9272 | 0.8429 | 0.9370 | 0.9289 | 0.8655 | 0.8246 |
| $CO_2$ (mol %) | 3.15 | 3.80 | 3.55 | 3.17 | 3.89 | 3.78 | 3.56 | 3.52 | 3.35 | 3.00 |
| CO (mol %) | 0.0592 | 0.0702 | 0.0804 | 0.0584 | 0.0594 | 0.0617 | 0.0649 | 0.0784 | 0.0587 | 0.0496 |
| $SO_2$ (mol %) | 14.9 | 12.0 | 13.7 | 11.5 | 13.4 | 12.5 | 11.8 | 14.0 | 17.2 | 15.6 |
| $H_2S$ (mol %) | 0.622 | 0.761 | 0.875 | 3.21 | 1.70 | 1.32 | 0.587 | 0.511 | 1.22 | 0.902 |
| $S_2$ (mol %) | 0.309 | 0.358 | 0.445 | 1.89 | 1.12 | 0.540 | 0.232 | 0.197 | 0.808 | 0.469 |
| COS (mol %) | 0.0013 | 0.0016 | 0.0022 | 0.0054 | 0.0032 | 0.0032 | 0.0013 | 0.0014 | 0.0026 | 0.0017 |
| HCl (mol %) | 0.1 | 0.171 | 0.153 | 0.167 | 0.148 | 0.162 | 0.151 | 0.174 | 0.169 | 0.173 |
| HF (mol %) | 0.19 | 0.20 | 0.12 | 0.20 | 0.19 | 0.17 | 0.15 | 0.19 | 0.18 | 0.17 |
| log $f(O_2)$ | -10.49 | -10.76 | -10.54 | -11.91 | -11.55 | -11.41 | -10.61 | -10.19 | -11.00 | -10.92 |
| log $f(Cl_2)$ | -12.05 | -11.95 | -11.97 | -12.41 | -12.36 | -12.23 | -12.00 | -11.71 | -12.02 | -11.97 |
| log $f(F_2)$ | -26.16 | -26.34 | -26.48 | -27.56 | -27.27 | -27.27 | -26.51 | -25.77 | -26.72 | -26.71 |

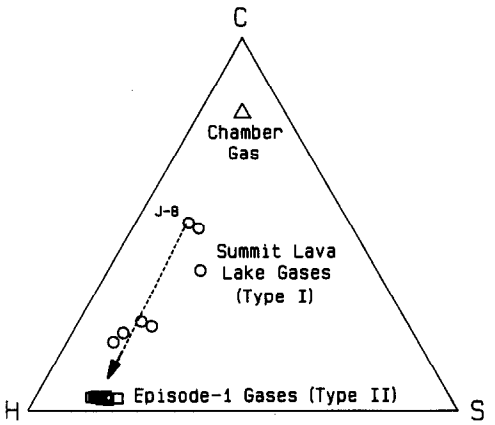


FIG. 3. Ternary plot of Type I volcanic gases (circles) from Table 1, Type II volcanic gases (squares) from Table 2, and a $CO_2$-rich summit chamber gas composition (triangle). The degassing vector originating at sample J-8 (Table 1) illustrates how the first-stage degassing of a $CO_2$-rich chamber gas (Fig. 2b) changes the gases magma emits upon eruption from Type I to Type II compositions, as discussed in the text. The ternary components are in mol% units defined as follows: C = $CO_2$ + CO; H = $H_2O$ + $H_2$ + HCl + HF; S = $SO_2$ + $H_2S$ + $S_2$.

gases. Type II volcanic gases like the episode 1 gases lie on a continuation of the summit lava lake degassing trend towards $CO_2$-depleted compositions (Fig. 3). The degassing vector in Fig. 3 illustrates how the first-stage degassing of a $CO_2$-rich chamber gas changes the gases magma emits upon eruption from Type I to Type II compositions. Thus, the episode 1 gases represent the second stage of degassing from magma that released excess $CO_2$ in summit chamber degassing earlier during equilibration to summit chamber pressures.

## OXYGEN BUFFERING OF KILAUEA VOLCANIC GASES

The foregoing results are consistent with the hypothesis that the episode 1 gases are equilibrium Type II volcanic gases at temperatures of 20–117°C above the collection temperatures. Strictly speaking, the chemical equilibrium demonstrated for the gases by the discussion in the Appendix is only an internal equilibrium state. It does not necessarily follow that the gases are in equilibrium with the lavas. In this section, I show that in these and other restored Kilauea gas compositions, the gas equilibrium is constrained by $f_{O_2}$ buffering related to transfer of oxygen from the gas to lava during cooling and that the equilibrium temperatures of the gases are the temperatures where this buffering ceased.

Plots of the log $f_{O_2}$ values of the restored episode 1 gas

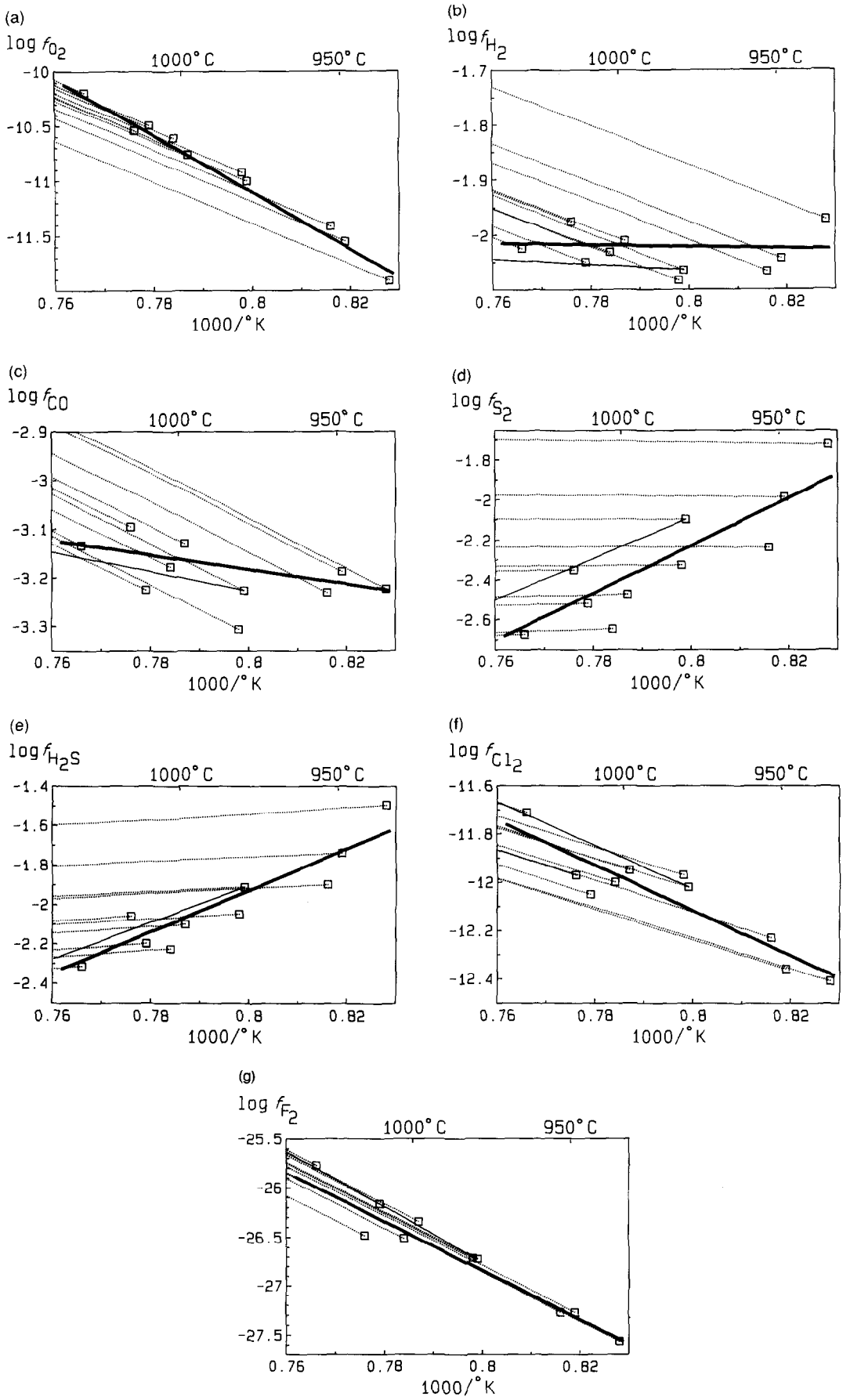
(a)
log $f_{O_2}$
1000° C
950° C
-10
-10.5
-11
-11.5
0.76
0.78
0.8
0.82
1000/° K
(b)
log $f_{H_2}$
1000° C
950° C
-1.7
-1.8
-1.9
-2
0.76
0.78
0.8
0.82
1000/° K
(c)
log $f_{CO}$
1000° C
950° C
-2.9
-3
-3.1
-3.2
-3.3
0.76
0.78
0.8
0.82
1000/° K
(d)
log $f_{S_2}$
1000° C
950° C
-1.8
-2
-2.2
-2.4
-2.6
0.76
0.78
0.8
0.82
1000/° K
(e)
log $f_{H_2S}$
1000° C
950° C
-1.4
-1.6
-1.8
-2
-2.2
-2.4
0.76
0.78
0.8
0.82
1000/° K
(f)
log $f_{Cl_2}$
1000° C
950° C
-11.6
-11.8
-12
-12.2
-12.4
0.76
0.78
0.8
0.82
1000/° K
(g)
log $f_{F_2}$
1000° C
950° C
-25.5
-26
-26.5
-27
-27.5
0.76
0.78
0.8
0.82
1000/° K

compositions (Table 2) against the reciprocal of absolute equilibrium temperatures show a linear trend (Fig. 4a). The correlation coefficient for log $f_{O_2}$ with $1/T$ is 0.991, and the coefficient of determination ($r^2$) is 0.982; thus, the variation in $1/T$ explains 98.2% of the variation in log $f_{O_2}$, and a least-squares linear regression of the data is justified. Because neither the log $f_{O_2}$ nor the $1/T$ variable was controlled during the investigation and since the data for both variables are subject to error, I have used the "two-error" linear regression method (YORK, 1969; LUDWIG, 1990), which gives the following result:

$$\log f_{O_2} = -26{,}410(1/T) + 10.06, \qquad (1)$$

where $f_{O_2}$ is in bars and $T$ is in degrees kelvin. The bold curve through the data points in Fig. 4a for the restored gas compositions (Table 2) is the linear regression curve based on Eqn. (1), and will be referred to as the "restored gas $f_{O_2}$ trend". A regression based only on the six equilibrium analyses (Pele 2, Pele 3, Pele 4, Pele 5, Pele 7, Pele 8) yields a result insignificantly different from Eqn. 1 at the 95% confidence level.

The linear restored gas $f_{O_2}$ trend in Fig. 4a is suggestive but not conclusive evidence that an external buffer controlled the oxygen fugacities of the episode 1 volcanic gases. It is possible, for example, that the restored gas $f_{O_2}$ trend represents the intrinsic $f_{O_2}$ of the volcanic gas phase during closed-system cooling and is unrelated to interaction with an external buffer. To investigate this possibility, equilibrium species distributions have been calculated for each of the samples by free energy minimization techniques (SMITH and MISSEN, 1982) from a representative eruption temperature for episode 1 of 1140°C down to the equilibrium temperatures implied by the gas compositions (Table 2). These calculations are constrained by the elemental compositions of the restored analyses given in Table 2, 1 bar total pressure, and thermochemical data from the 1985 JANAF tables (CHASE et al., 1985). The calculations model the equilibrium species distributions of the gas phase during closed-system cooling, i.e., without external buffering. The intrinsic log $f_{O_2}$ values calculated for closed-system cooling are plotted as dotted curves for each sample in Fig. 4a. The intrinsic log $f_{O_2}$ cooling paths of the individual samples deviate consistently from the restored gas $f_{O_2}$ trend. Thus, some form of external $f_{O_2}$ buffering is indicated, unless the linear distribution of points in Fig. 4a is entirely fortuitous. Perhaps homogeneous reaction equilibria in the gas phase were quenched at various temperatures during closed-system cooling that by chance just happened to form the linear array of points in Fig. 4a. This "explanation" is not very satisfying. It does not explain why the intrinsic $f_{O_2}$ cooling curves of the samples are dissimilar and spread out over a half order of magnitude at temperatures between 1032 and 935°C, even though similar curves are expected since the gases are presumably from the same source and, in some cases, were collected within minutes of each other.

I propose that the deviations of the intrinsic $f_{O_2}$ cooling paths from the restored gas $f_{O_2}$ trend result from oxygen fugacity buffering of the episode 1 gases by oxygen transfer from the major species in the gas phase ($H_2O$, $CO_2$, $SO_2$) to the lava during open-system cooling. The gentler slopes of the intrinsic $f_{O_2}$ cooling curves compared to the slope of the restored gas $f_{O_2}$ trend suggest that the gases tend to become oxidizing relative to the lavas during cooling. This tendency is consistent with the high $SO_2$ contents of the episode 1 gases (GERLACH and NORDLIE, 1975b). Upon cooling, $SO_2$ reacts with $H_2$ to form $H_2S$ and $H_2O$, thus increasing $H_2O/H_2$. In the $H_2O$-rich episode 1 gases, shift in the $H_2O/H_2$ exerts a first-order control on the bulk gas $f_{O_2}$. Increasing $H_2O/H_2$ by reaction of $SO_2$ with $H_2$ thus leads to a higher $f_{O_2}$ for the gas and a greater potential for oxygen transfer to the lava than would be true if the episode 1 gases contained less $SO_2$. The gas samples with lower equilibrium temperatures have lost more oxygen to the lavas through buffering down to lower temperatures, and have lower relative intrinsic $f_{O_2}$'s as a result. Thus, the spread in the relative intrinsic $f_{O_2}$ curves of the gas samples over about a half order of magnitude is caused by the transfer of variable amounts of oxygen from the gas phase to the lavas during buffering. By this interpretation, the equilibrium temperatures obtained in the thermodynamic analysis of the episode 1 gas data presented in the Appendix represent the temperatures at which the oxygen transfer from the gas phase to the lavas ceased. Short-term fluctuations in gas flow rates probably cause the observed variability in oxygen transfer and equilibrium temperatures. Higher flow rates restrict the time available for gas/lava interactions and result in gas samples with higher equilibrium temperatures and higher relative intrinsic oxygen fugacities; lower flow rates permit more time for cooling and oxygen transfer, resulting in lower equilibrium temperatures and lower relative intrinsic oxygen fugacities. The fact that the restored gas $f_{O_2}$ trend is preserved in the samples suggests that homogeneous reaction rates in the gas phase are slow relative to the time it took for the gases to move from the last site of gas/lava buffering by oxygen transfer to the site of collection. As shown in the Appendix, moreover, the episode 1 gases show no evidence that certain groups of gas species are kinetically more responsive and equilibrate homogeneously down to lower temperatures (NORDLIE, 1971; GIGGENBACH, 1987).

Alternative processes for buffering the gases by adding reduced forms of C, H, and S to the gas phase during cooling seem less plausible. Mechanisms for transferring reduced forms of C and S from the lava to the gas phase at the pace required to maintain redox equilibrium during cooling are not readily apparent. Furthermore, the lavas involved are largely degassed and contain only residual amounts of dissolved C, H, and S volatiles that seem insubstantial for buffering the larger volatile mass in the gas phase and that have greatly diminished potentials for escaping into the gas. $H_2$ diffusion may be a viable mechanism, but the only plausible

FIG. 4. $Log_{10}$ fugacity vs. reciprocal absolute temperature for the species $O_2$, $H_2$, CO, $S_2$, $H_2S$, $Cl_2$, $F_2$. Bold lines represent restored gas trends based on least-squares regressions of restored gas composition data from Table 2. Dotted lines show equilibrium intrinsic log $f_i$ paths during closed system cooling from high temperatures to the last equilibrium temperature (Table 2). The solid lines (b–g) show examples based on Pele 8 of equilibrium log $f_i$ paths during open system cooling with $O_2$ fugacity constrained by Eqn. 1.

source of $H_2$ would seem to be the reduction of residual water in the melt (glass) by ferrous iron (SATO, 1978). This process, which requires breakdown of residual water in melt (glass) by iron redox reactions, in addition to $H_2$ transfer by diffusion through the melt (glass) and into the gas phase, seems more complicated than one based simply on the transfer of oxygen from the gas to the lava by iron redox reactions. The mechanism for promoting $H_2$ diffusion depends, moreover, on the activity of $H_2O$ in the residual melt/glass. At the low bulk residual water contents ($\approx$0.1 wt%) of subaerial Kilauea melt (glass) (GERLACH and GRAEBER, 1985), the activity of molecular $H_2O$ is extremely low, and almost all water in silicate melt is dissolved as OH groups (STOLPER, 1982). CARMICHAEL (1991) suggests that under such conditions, the generation and diffusive loss of $H_2$ by dissociation of dissolved $H_2O$ is insignificant.

The fugacity trends of several minor and trace species (Fig. 4b–g) support the inference that $f_{O_2}$ buffering of the episode 1 gases occurred by transfer of oxygen from the gas phase to lava during cooling. The restored gas fugacity trends indicated by bold linear regression curves for the samples have distinctly different slopes than the slopes of the intrinsic fugacities (dashed curves) during closed system cooling of the individual samples, except in the case of $F_2$ (Fig. 4b–g). However, when equilibrium cooling curves for the individual samples are calculated with a computer code (RANDICH and GERLACH, 1981) that adjusts their elemental oxygen contents to give $O_2$ fugacities constrained by Eqn. 1, in order to simulate open system cooling with gas/lava oxygen transfer, the slopes mimic the slopes of the restored gas fugacity trends. This effect is illustrated by the solid curve for Pele 8 in Fig. 4b–g. The open system, $f_{O_2}$-buffered cooling curves for the other samples all show similar trends to those of Pele 8; to keep Fig. 4b–g legible, only the open system curve for Pele 8 is shown. The results indicate that $f_{O_2}$ buffering by oxygen transfer from the gas phase to the lavas during cooling controlled the fugacities of the minor and trace species of the gases. The role of $f_{O_2}$ buffering in controlling the fugacity of $F_2$ (Fig. 4g) is ambiguous; the restored gas $f_{F_2}$ trend, the intrinsic $f_{F_2}$ cooling paths, and the open system $f_{F_2}$ cooling paths with gas/lava oxygen transfer are all parallel.

It is perhaps noteworthy that the restored gas fugacity trend for $H_2$ (Fig. 4b) is approximately constant ($\log f_{H_2} \approx -2$). This feature might be viewed as evidence for control of $f_{O_2}$ by the high effusive mobility of $H_2$ producing a uniform $f_{H_2}$ across the temperature gradient in the spatter-covered fissure. However, the fugacity trend for $H_2$ is also constant during simulated open system cooling of Pele 8 with its $f_{O_2}$ buffered by oxygen transfer from the gas phase to lava with falling temperature. Indeed, thermodynamic calculations show that any gas containing about 80% $H_2O$, like the episode 1 gases (Table 2), with its $f_{O_2}$ constrained by Eqn. 1 will have $\log f_{H_2}$ values of approximately $-2$ from 1035–935°C. Constant $f_{H_2}$ is a thermodynamic inevitability over this temperature range for any water-rich volcanic gas with its $f_{O_2}$ buffered along a $\log f_{O_2}$-reciprocal temperature slope similar to that defined by Eqn. 1, regardless of the buffering mechanism. For example, C-O-H-S gases containing 80% water and buffered along FMQ have $\log f_{H_2}$ values of about $-1.8$ in this temperature range; buffering along nickel-nickel oxide (NNO) gives $\log f_{H_2}$ values of about $-2.3$.

The Type I volcanic gases in Table 1 are based on restored gas compositions (GERLACH, 1980) obtained from summit lava lake gas analyses by the same procedures employed in the Appendix to interpret and correct the analytical data for the episode 1 gases. The restored summit lava lake Type I gas compositions define a restored gas $f_{O_2}$ curve that lies on the same trend as the $f_{O_2}$ curve for the restored episode 1 Type II gases (Fig. 5). Indeed, the correlation coefficient for the combined data sets is 0.9975, and 99.5% of the variation in $\log f_{O_2}$ is accounted for by variation in $1/T$ ($r^2 = 0.995$). It can be shown, moreover, that, as in the case of the episode 1 gases, the intrinsic $O_2$ fugacities of the individual Type I restored gas compositions also follow paths that lead to higher values during closed system cooling than the values along the restored gas $f_{O_2}$ trend, just as in Fig. 4a; when compared at a common temperature, the intrinsic $O_2$ fugacities for both data sets range over an order of magnitude. I infer from these relationships that the gas/lava oxygen transfer proposed above for buffering the $f_{O_2}$ of the episode 1 Type II gases also operates in molten lava up to 1185°C and is responsible for the restored gas $f_{O_2}$ trend of the Type I summit lava lake gases.

Combining the $1/T$ and $\log f_{O_2}$ values from both data sets (Tables 1 and 2) in a least-squares linear regression by the two-error method (YORK, 1969; LUDWIG, 1990) gives the following equation for the $O_2$ fugacity of Kilauea gases from 1185–935°C:

$$\log f_{O_2} = -24{,}200(1/T) + 8.30. \quad (2)$$

Equation 2 is plotted in Fig. 5 along with the 95% confidence level error envelope for the regression line. Thus, the probability that the true regression line will fall somewhere within the area defined by the envelope is 0.95. The error envelope is very small because of the low level of scatter in the data

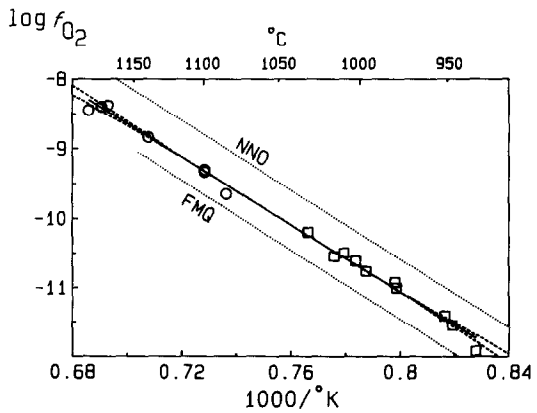


FIG. 5. $\text{Log}_{10} f_{O_2}$ vs. reciprocal absolute temperature for summit lava lake Type I volcanic gases (circles) and episode 1 Type II volcanic gases (squares). The $\log f_{O_2}$ and temperature values are for the restored gas compositions in Tables 1 and 2. The solid line is the Eqn. 2 linear regression line for the Type I and Type II gases. The dashed line is the 95% confidence level error envelope for the regression line. NNO is the nickel-nickel oxide buffer of HUEBNER and SATO (1970). FMQ is the fayalite-magnetite-quartz buffer of O'NEILL (1987), which is not calibrated at temperatures above 1147°C.

and the excellent fit to a linear regression model. The error envelope was calculated from the 95% confidence limits for the slope and intercept of Eqn. 2 (±1.2 and ±0.91, respectively), the mean $1/T$ of the data (0.00076), and equations given by LUDWIG (1980). The regression analysis was carried out with software developed by LUDWIG (1990) that evaluates the proportion of scatter from a straight line that is attributable to the levels of error expected in the log $f_{O_2}$ and $1/T$ data. The results indicate that all the scatter is accounted for by the realistic error assignments of ±10°C in $T$ and ±0.1 in log $f_{O_2}$.

Equation 2 differs from the $O_2$ fugacity curve obtained previously from calculations based on analyses of several gas samples from the Puu Oo eruption (GREENLAND, 1988). The analyses used in the earlier work were not equilibrium compositions, and no systematic effort was made to identify the causes of disequilibrium and to restore them before the $f_{O_2}$ calculations were made. The results show considerably more scatter (about 1 log unit in $f_{O_2}$) than those in Fig. 5. Although it is questionable just how comparable the results are to the demonstrated equilibrium values in Fig. 5, they produce a least-squares linear regression line that gives log $f_{O_2}$ values about half an order of magnitude lower than those of Eqn. 2 at 1185°C and about half an order of magnitude higher at 935°C.

Oxygen fugacity measurements on residual volcanic gases provide a test of Eqn. 2 for subsolidus conditions. Residual gases are the gases remaining in lavas after eruptive subaerial degassing. Residual gases at Kilauea are $H_2O$-rich with trace amounts of $CO_2$, $SO_2$, $H_2$, and $H_2S$ (GERLACH, 1980). These gases escape from flowing lava but are normally so diluted by air that uncontaminated samples are difficult to obtain. Ponded lava flows provide environments where residual gases can develop in concentrated enough amounts to be studied. Measurements of the oxygen fugacity of residual gases flowing into drill holes into the hot crust of Makaopuhi lava pond, which formed approximately 4 km up rift from the location of Vent B (Fig. 1) during an eruption that began on 5 March 1965, are among the most successful examples of such studies (SATO and WRIGHT, 1966; WRIGHT and OKAMURA, 1977).

Oxygen fugacity measurements were initiated with an oxygen probe in drill holes about three months after the eruption began. The probe was used with good reproducibility through September 1965 when fluctuating EMF began to cause erratic measurements (WRIGHT and OKAMURA, 1977). All holes eventually developed high $f_{O_2}$ zones due to oxidation processes occurring in the lava lake crust. SATO and WRIGHT (1966) attributed the high $f_{O_2}$ zones to preferential escape of $H_2$ by diffusion from certain horizons of the lake, although WRIGHT and OKAMURA (1977) found this hypothesis less tenable than one based on the circulation of air-saturated rainwater. Nevertheless, most drill holes showed "normal profiles" at some interval of time when log $f_{O_2}$ varied linearly with the reciprocal of absolute temperature (WRIGHT and OKAMURA, 1977). Over the period of reliable probe performance, drill holes 9 and 10 developed normal profiles with the lowest observed $f_{O_2}$ values, suggesting that these holes were the least influenced by oxidation processes (SATO and WRIGHT, 1966). The twenty-three normal $f_{O_2}$ values obtained at temperatures from 963–538°C in drill holes 9 and 10 from 30 June 1965, when measurements began in drill hole 9, through 23 September 1965, when oxidation effects began to show in both holes, are plotted in Fig. 6 along with the values for the Type I and Type II restored gas compositions (Table 1 and 2). Figure 6 also includes the Eqn. 2 regression line for the oxygen fugacity of Kilauea gases and the 95% confidence level error envelope for Eqn. 2 projected down to the lowest temperatures of the drill hole data.

The data for the residual gases show more scatter than the restored gas compositions (Fig. 6). Assigned errors of ±10°C in $T$ and ±0.1 in log $f_{O_2}$, which account for all the scatter from a straight line in the restored gas composition values, account for only a minor fraction of the scatter in the data for the residual gases. Nevertheless, about 25% of the measured residual gas oxygen fugacities falls within the error envelope for Eqn. 2, and the remaining 75% is just slightly above it, presumably because of modest but variable oxidation by secondary processes. The $f_{O_2}$-$T$ data for the residual gases suggest that gas-to-lava oxygen transfer for buffering the oxygen fugacity of Kilauea gases operated down to at least 538°C, probably aided by the much lower flow rates of residual gases, compared to Types I and II eruptive gases, which provides more time for oxygen transfer to occur at lower temperatures. Nevertheless, it is clear that Eqn. 2 will in general underestimate the $f_{O_2}$ of residual gases emitted by lava flows and lava ponds, except in the initial stages of cooling when oxidation by secondary processes is minor. Unsurprisingly, the higher temperature (earlier) residual gas oxygen fugacity values agree better with the predicted values from Eqn. 2. It is noteworthy that the initial oxides from Makaopuhi lava lake give a log $f_{O_2}$ of −10.5 and a temperature of 1020°C (WRIGHT and WEIBLEN, 1968), which is in excellent agreement with the value of −10.42 predicted by Eqn. 2 at 1020°C.

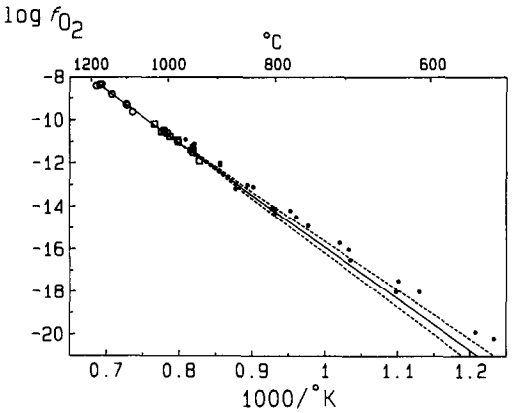


FIG. 6. $Log_{10} f_{O_2}$ vs. reciprocal absolute temperature for summit lava lake Type I volcanic gases (large circles, Table 1), episode 1 Type II volcanic gases (squares, Table 2), and the residual volcanic gases (small dots) from drill holes 9 and 10 into the crust of Makaopuhi lava lake (SATO and WRIGHT, 1966; WRIGHT and OKAMURA, 1977). The solid line is the Eqn. 2 linear regression line for the Type I and Type II gases. The dashed line is the 95% confidence level error envelope for the regression line.

Gas/lava equilibration may be a common process in erupting lavas. Chemical data for fumarolic discharges at White Island, for example, show evidence of heterogeneous equilibrium (GIGGENBACH, 1987). Gas/lava equilibration by oxygen exchange should, therefore, be considered when modeling volcanic gas compositions over a range of temperatures. The usual practice of simply calculating equilibrium species distributions at temperatures of interest constrained only by the bulk elemental composition of a gas analysis may be misleading if oxygen exchange processes alter the bulk elemental content of the gas and buffer its $f_{O_2}$ as temperature changes. To properly estimate the compositions of the episode 1 gases at a realistic eruption temperature, it is necessary to calculate the species distributions from the bulk elemental compositions given for the gas samples in Table 2 at 1140°C with enough oxygen added to the analyses to satisfy the $f_{O_2}$ buffering constraint defined by Eqn. 2 for that temperature. Table 3 shows a comparison of $f_{O_2}$-buffered and $f_{O_2}$-unbuffered species distributions at 1140°C and 1 bar total pressure for Pele 8. Significant differences are apparent in the $f_{O_2}$'s and in the concentrations of $H_2$, CO, $H_2S$, and $S_2$ in the distributions.

Although the details of the $f_{O_2}$ buffering mechanisms for oxygen transfer are unknown, the fact that $f_{O_2}$ buffering is effective from molten to subsolidus conditions suggests that the reaction mechanisms change with cooling as the reactants change from predominantly melt, to melt plus crystals, to glass plus crystals. Changes in the slope of the log $f_{O_2}$-$1/T$ curve may also accompany the changes in the identity of the reactants, but at a scale unresolvable in the gas data. Mass balance calculations based on Pele 8 indicate that heterogeneous ferrous/ferric redox reactions are plausible mechanisms for the oxygen transfer required by the $f_{O_2}$ buffering of the episode 1, gases and that the oxygen fugacity of Kilauea volcanic gases is consistent with sliding ferrous/ferric equilibria in the erupting lavas. A Kilauea basalt containing 0.28 wt% $H_2O$, 0.02 wt% $CO_2$, and 0.09 wt% S prior to degassing would produce a Type II volcanic gas with a composition similar to Pele 8, assuming that the residual volatile contents for the lava are 0.10 wt% $H_2O$, <0.001 wt% $CO_2$, and 0.015 wt% S. These pre-eruptive and residual concentrations are based on earlier work (GERLACH and GRAEBER, 1985; GREENLAND et al., 1985; GERLACH, 1986) and require the degassing of about 2150 g of magma to produce the 7.52 g sample weight of Pele 8. For purposes of illustration, an initial $FeO/Fe_2O_3$ of 4.52 (weight) is assumed for the erupted lava, based on the data of WALLACE and CARMICHAEL (1992) for a basalt glass (sample HVO-674) from the current Puu Oo eruption. The MgO-glass geothermometer for Kilauea glasses (HELZ and THORNBER, 1987) indicates a temperature of 1142°C for HVO-674 (WALLACE and CARMICHAEL, 1992), which is within the range of higher temperature episode 1 lavas. At this temperature, the $Fe_2O_3/FeO$ glass geobarometer (KRESS and CARMICHAEL, 1991) gives a log $f_{O_2}$ value of −8.73 (WALLACE and CARMICHAEL, 1992), which agrees well with the log $f_{O_2}$ of −8.80 predicted at 1142°C from Eqn. 2. To satisfy $f_{O_2}$ constraints, the computer calculations simulating gas/lava oxygen transfer require the removal of 0.0167 mol of elemental oxygen from Pele 8 during cooling from a representative episode 1 eruption temperature of 1140°C down to its last equilibrium temperature of 979°C, which is approximately the solidus temperature of Kilauea basalt (HELZ and THORNBER, 1987). Assuming the oxygen transfer is accomplished by oxidation of ferrous iron in lava with the above initial $FeO/Fe_2O_3$ of 4.52, the resulting $FeO/Fe_2O_3$ is 4.24, a decrease from the initial value of a mere 6%. It should be kept in mind that the initial $FeO/Fe_2O_3$ of the lava is likely to be higher than the value based on HVO-674 glass in this illustration because of possible secondary oxidation effects in the erupted glass and the presence of FeO in associated olivine crystals. Thus, from a mass balance perspective alone, heterogeneous ferrous/ferric redox reactions in Kilauea basalt appear to be fully adequate to transfer the quantity of oxygen from gas to lava required by $f_{O_2}$ buffering of the gas phase during cooling.

Table 3. Species distributions for Pele 8 at 1140 °C

| | buffered[a] | unbuffered |
|---|---|---|
| $H_2O$ | 75.8[b] | 75.3 |
| $H_2$ | 0.9582 | 1.781 |
| $CO_2$ | 3.26 | 3.23 |
| CO | 0.0912 | 0.169 |
| $SO_2$ | 19.4 | 17.5 |
| $H_2S$ | 0.156 | 0.918 |
| $S_2$ | 0.0773 | 0.772 |
| COS | 0.00049 | 0.0029 |
| HCl | 0.166 | 0.168 |
| HF | 0.18 | 0.18 |
| log $f_{O2}$ | -8.82 | -9.27 |
| log $f_{Cl2}$ | -11.18 | -11.44 |
| log $f_{F2}$ | -24.16 | -24.41 |

[a] $f_{O2}$ constrained by (2) at 1140 °C
[b] mol % concentrations

## Gas/Lava Exchange of Other Volatile Components

The buffering of $f_{O_2}$ by oxygen transfer between the gas phase and lava during cooling of the episode 1 gases exerted a primary control on the fugacities of minor and trace species. Although the possible role of gas/lava exchanges of other volatile components (C, H, S, Cl, F) in controlling the restored gas fugacity trends during cooling cannot be entirely ruled out, it appears from the results in Fig. 4b–g that such exchanges, compared to oxygen exchange, exerted only minor influences (if any) on the episode 1 gases at temperatures below 1032°C (the highest equilibrium temperature determined for the episode 1 gas samples). Thus, while the episode 1 lavas and gases approached chemical equilibrium during cooling with respect to oxygen, it is not as obvious that they did so with respect to other volatile components. At temperatures above 1032°C, however, exchanges of other components in addition to oxygen become increasingly likely to occur. It is of interest, therefore, to compare the fugacity trends of species other than $O_2$ in the higher temperature Type I gases (Table 1) with those of the episode 1 gases. Unfortunately, such a comparison is complicated by the large differences in bulk composition between the two sets of data (Fig. 3) and among the Type I gases themselves, which reflect sampling of variably degassed lava on a one sample per site

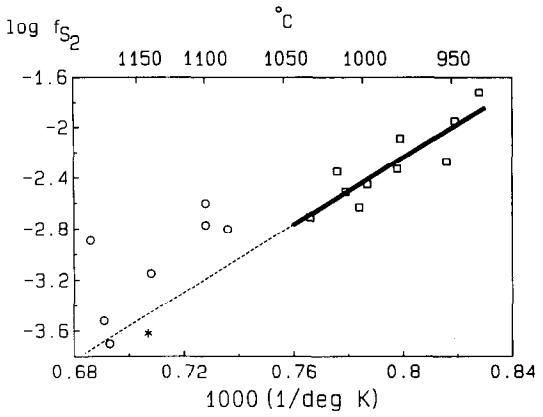


FIG. 7. $\text{Log}_{10} f_{S_2}$ vs. reciprocal absolute temperature for summit lava lake Type I volcanic gases (circles) and episode 1 Type II volcanic gases (squares). The log $f_{S_2}$ and temperature values are for the restored gas compositions in Tables 1 and 2. Bold line represents restored gas trend for episode 1 gases based on least-squares regressions of restored gas composition data from Table 2. Dashed line is extrapolation of trend for episode 1 gas data to higher temperatures. Asterisk represents calculated log $f_{S_2}$ for Kilauea basalt glass HVO-674 (WALLACE and CARMICHAEL, 1992).

basis from several locations around a summit lava lake. Nevertheless, the Type I samples have similar total sulfur contents to the episode 1 gases, suggesting fugacity trends for $S_2$ may be comparable. The results in Fig. 7 indicate the $S_2$ fugacities of the Type I gases tend to lie above the extrapolated $f_{S_2}$ trend of the episode 1 gases, although the agreement is good for a few samples. The $S_2$ fugacity calculated by WALLACE and CARMICHAEL (1992) for a Kilauea basalt glass (HVO-674) at 1142°C and containing 100 ppm residual sulfur agrees well with the extrapolated $f_{S_2}$ trend of the episode 1 gases (Fig. 7). These results are too sparse to draw any final conclusions, but a preliminary interpretation is that gas/lava exchange of sulfur occurs early in the degassing process at eruption temperatures and that gas/lava exchange of oxygen becomes the main control on $S_2$ fugacity at some later time during cooling. Thus, the gas phase and the melt phase probably approach equilibrium with respect to sulfur distribution at the low pressures and temperatures of the erupting lava (WALLACE and CARMICHAEL, 1992) but do not maintain equilibrium during later cooling.

## OXYGEN FUGACITY OF KILAUEA BASALT

### $f_{O_2}$ of Subaerial Lavas

The evidence discussed above indicates that subaerial lavas buffer volcanic gas compositions emitted by Kilauea basalt along a consistent $f_{O_2}$-$T$ trend from molten to subsolidus temperatures. Because gas reaction equilibria are preserved in the gas phase when oxygen transfer between gas and lava ceases, the $f_{O_2}$ of Kilauea volcanic gases can be used to calibrate the $f_{O_2}$ of coexisting Kilauea basalt. Thus the equilibrium $f_{O_2}$-$T$ relationship defined by Eqn. 2 provides an oxygen fugacity geobarometer for fresh, unaltered Kilauea basalt from liquidus to subsolidus temperatures in surface and shallow environments during and immediately following subaerial eruptions. Whether or not the gas calibrated oxygen fugacity is also the equilibrium oxygen fugacity of Kilauea basalt is debatable. It may be a good estimate of the equilibrium oxygen fugacity of Kilauea basalt at temperatures well above the solidus (e.g., >1100°C), but it almost certainly will deviate from true equilibrium below the solidus because mineral assemblages are not well equilibrated in rapidly cooled Kilauea flows (R. Helz, pers. commun., Sept. 1991).

The oxygen fugacity of subaerial Kilauea basalt as defined by Eqn. 2 is about midway between FMQ (O'NEILL, 1987) and NNO (HUEBNER and SATO, 1970) (Fig. 5). Equation 2 is strictly applicable for temperatures from 1185–935°C and thus covers a range from the liquidus temperature of Kilauea basalt containing about 8.5 wt% MgO to below the solidus temperature of 980 ± 10°C (HELZ and THORNBER, 1987). Over this temperature interval, the $f_{O_2}$ of Kilauea basalt relative to NNO, $\Delta_{NNO}$ = log $f_{O_2}$ (Eqn. 2)–log $f_{O_2}$ (NNO), ranges from −0.56 (1185°C) to −0.46 (935°C). Extensions above 1185°C to the liquidus temperatures of more MgO-rich Kilauea basalts should be made with caution, but extensions up to 1300°C seem justified by the consistency of the data from 935–1185°C. The data discussed above for residual volcanic gases (Fig. 6) suggest that Eqn. 2 is valid down to about 500°C, but only if the basalt in question is unaffected by oxidation during cooling. The relative $f_{O_2}$ of Kilauea basalt, as defined by $\Delta_{NNO}$, increases as temperature decreases and becomes zero at about 415°C.

Several factors suggest confidence in the gas-based approach used here to estimate the oxygen fugacity of subaerial Kilauea basalt from liquidus to subsolidus conditions. The approach is based on validated equilibrium compositions for Type I and Type II gases whose oxygen fugacities are demonstrably constrained by interactions with lava. The approach differs in this regard from most conventional petrologic approaches in which equilibrium is assumed at the outset and $O_2$ fugacities are calculated directly from mineral and/or glass analytical data without testing the validity of the equilibrium assumption. The excellent fit of the two restored gas data sets to a linear regression oxygen fugacity model is noteworthy in view of how little the two data sets have in common. One data set covers magmatic temperatures up to liquidus temperatures; the other data set covers temperatures ranging over 50°C on either side of the solidus temperature. Thus, the range of crystal/melt proportions encompassed by the gases employed in this study is much greater than that represented by the mineral/glass assemblages employed in most conventional petrologic studies of the oxygen fugacity of basalts; magnetite-ilmenite geothermometry, for example, cannot be used above the temperature of incoming magnetite in Kilauea basalt, which is about 1090°C (THOMPSON and TILLEY, 1969; HELZ and THORNBER, 1987). The two data sets also cover a wide range of gas compositions, as is evident from Fig. 3 and Tables 1 and 2. They involve, moreover, two very different degassing histories: (1) direct, one-stage, sustained eruptive degassing in the case of the Type I summit lava lake gases, and (2) quiescent summit chamber degassing followed by a long period of storage in Kilauea's magma reservoir complex (during which second boiling related to crystallization may have caused further minor degassing) with a second stage of eruptive degassing in an ERZ eruption in the case of the Type II episode 1 gases. It is also noteworthy

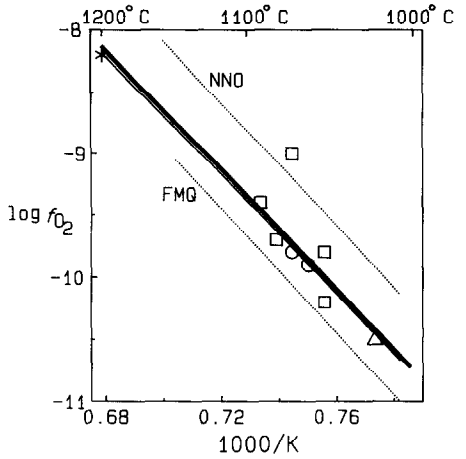


FIG. 8. $Log_{10}$ $f_{O_2}$ vs. reciprocal absolute temperature for Kilauea basalts. The bold line is Eqn. 2 of this study based on the Type I and Type II volcanic gases. The asterisk is the $f_{O_2}$ determined experimentally by FUDALI (1965) for a 1921 lava flow. The triangle is based on the initial Fe-Ti oxides from Makaopuhi lava lake (WRIGHT and WEIBLEN, 1968). The circles are based on the initial Fe-Ti oxides from Kilauea Iki lava lake (ANDERSON and WRIGHT, 1972). Squares represent estimates based on Fe-Ti oxides in hybrid lavas (ANDERSON and WRIGHT, 1972). The thin solid line is based on a least-squares regression of all the basalt data except the hybrid lava with $f_{O_2}$ above NNO. NNO is the nickel-nickel oxide buffer of HUEBNER and SATO (1970). FMQ is the fayalite-magnetite-quartz buffer of O'NEILL (1987), which is not calibrated at temperatures above 1147°C.

that completely different collection and analytical techniques were used to obtain the two sets of data.

The $f_{O_2}$ of subaerial Kilauea basalt predicted by Eqn. 2 is consistent with previous estimates (Fig. 8) based on Fe-Ti oxides and $Fe_2O_3$/FeO in glassy Kilauea lavas. Equation 2 predicts a log $f_{O_2}$ value of −8.13 at 1200°C, which agrees well with an experimentally determined value of −8.2 at 1200°C for a 1921 Kilauea lava flow (FUDALI, 1965). Although it is unclear whether the $Fe_2O_3$/FeO of the 1921 lava flow is pristine (R. Helz, pers. commun., Sept. 1991), SATO and MOORE (1973) report that the value of FUDALI (1965) is consistent with results obtained at 1200°C on Kilauea basalt by the oxygen cell method. Several results from past studies of Fe-Ti oxides in mixed and fractionated Kilauea lavas (ANDERSON and WRIGHT, 1972) and of the initial oxides crystalized in Makaopuhi lava lake and Kilauea Iki lava lake (WRIGHT and WEIBLEN, 1968; ANDERSON and WRIGHT, 1972) are presented in Fig. 8. Except for one hybrid lava, the Fe-Ti oxide results are in good agreement with Eqn. 2. Several of the hybrid lavas studied by ANDERSON and WRIGHT (1972) give Fe-Ti oxide temperatures above 1100°C, which is too high for magnetite crystallization in Kilauea basalt (THOMPSON and TILLEY, 1969; HELZ and THORNBER, 1987). Reinterpretation of the oxide data in ANDERSON and WRIGHT (1972) with the revised $f_{O_2}$-$T$ grid of SPENCER and LINDSLEY (1981) leads to similar results, suggesting that Fe-Ti oxides in many of the hybrid lavas have complex histories and may not be equilibrated. The results for hybrid lavas from ANDERSON and WRIGHT (1972) presented in Fig. 8 are restricted to samples giving Fe-Ti oxide temperatures less than 1100°C. Finally, Eqn. 2 predicts $\Delta_{NNO}$ values about half an order of magnitude higher than the average calculated by CARMICHAEL and GHIORSO (1986) from application of a glass $f_{O_2}$ geobarometer to published analyses of $Fe_2O_3$ and FeO in glassy Kilauea lavas. The $\Delta_{NNO}$ values obtained from Eqn. 2 are, nevertheless, within the margin of error of the geobarometer used by CARMICHAEL and GHIORSO (1986). The tendency for the glass geobarometer to give somewhat lower values than Eqn. 2 may reflect contributions of FeO from olivine crystals that are usually present in glassy Kilauea lavas. The highest $\Delta_{NNO}$ values obtained by I. S. E. Carmichael and M. S. Ghiorso (Fig. 1; CARMICHAEL, 1991), which presumably are least affected by FeO from olivine, are in excellent agreement with Eqn. 2, as is the result obtained for the Kilauea glass (HVO-674) discussed previously.

## MgO Glass Geobarometer

Combining Eqn. 2 with the glass geothermometer of HELZ and THORNBER (1987) permits estimation of the $f_{O_2}$ of glassy subaerial Kilauea basalts from the MgO content of unaltered glass coexisting with olivine. HELZ and THORNBER (1987) derived the following empirical geothermometer from melting experiments on Kilauea glasses:

$$T = 20.1\ \mathrm{MgO} + 1{,}014, \qquad (3)$$

where $T$ is in °C, and MgO is the wt% MgO content of the glass. This calibration is applicable only to unaltered glass coexisting with olivine and holds from liquidus temperatures down to 1030°C, or about 1 wt% MgO (HELZ and THORNBER, 1987). Converting $T$ in Eqn. 3 to absolute temperature and combining with Eqn. 2 gives the following expression for oxygen fugacity:

$$\log f_{O_2} = \frac{-24{,}200}{20.1\ \mathrm{MgO} + 1{,}287} + 8.30. \qquad (4)$$

Equation 4 provides an empirical geobarometer for estimating the oxygen fugacity of Kilauea vent spatter, tephra, and glassy subaerial lavas above 1030°C, provided that the glass coexists with olivine. The advantage of the glass MgO geobarometer over most mineralogical $f_{O_2}$ geobarometers is its applicability up to liquidus temperatures, and it does not necessitate determination of ferrous/ferric data required by glass $f_{O_2}$ geobarometers. It can only be used, however, to estimate the $f_{O_2}$ of lavas during subaerial eruption or in the early stages of cooling in surface and near-surface environments. The total uncertainty for temperature estimates by Eqn. 3 is ±10°C (HELZ and THORNBER, 1987), which implies uncertainties in log $f_{O_2}$ by Eqn. 4 of ±0.10 at 1300°C and ±0.15 at 1030°C. Like Eqn. 3, Eqn. 4 may prove applicable to Mauna Loa glasses (HELZ and THORNBER, 1987).

## Source Region versus Degassing Control of $f_{O_2}$

The oxygen fugacity of Kilauea basalt is unknown in its mantle source region, during its transport through the mantle, and upon its arrival in the crust prior to degassing in the summit chamber. The data available for the isotopic composition of sulfur in submarine lavas from the ERZ indicate that 13–36% of the sulfur in these Kilauea basalts is present as sulfate, the remainder being sulfide (SAKAI et al., 1982). This redox state for dissolved sulfur in basaltic liquid cor-

responds to oxygen fugacities between NNO and FMQ (KATSURA and NAGASHIMA, 1974; CARROLL and RUTHERFORD, 1988), which suggests that the $f_{O_2}$ of ERZ submarine basalt after summit chamber degassing and prior to eruption is within ±0.5 log units of the subaerial values defined by Eqn. 2. Furthermore, sulfate sulfur comprises about the same proportion of the residual sulfur in subaerial Kilauea basalt (SAKAI et al., 1982; WALLACE and CARMICHAEL, 1992) as it does in the ERZ submarine lavas, which suggests that the $f_{O_2}$ of Kilauea basalt stored in the crust is similar to that of subaerially erupted basalt and probably well approximated by Eqn. 2. Thus, the oxygen fugacity of Kilauea basalt stored in the crust is apparently consistent with the range of $f_{O_2}$ values between FMQ and NNO that have been inferred both for ocean island basalts from their spinels and for the source regions of ocean island basalts from the spinels in their mantle xenoliths (MATTIOLI et al., 1989; BALLHAUS et al., 1990). The consistency of results supports the hypothesis that the oxygen fugacities of basaltic magmas are inherited from their mantle source regions (CARMICHAEL, 1991).

Some models, however, would have basalt generated in mantle source regions at oxygen fugacities much lower than those of the subaerial lavas (SATO, 1978; MATHEZ, 1984). For these models to be consistent with the $f_{O_2}$ of subaerial Kilauea basalt, oxidation must take place during ascent from the mantle and/or storage in the crust. SATO (1978) proposed that degassing by $H_2$ diffusion during mantle ascent and storage in the crust causes oxidation and gives rise to subaerial basalts with higher $f_{O_2}$ than their mantle source regions. MATHEZ (1984) proposed that fractional degassing of CO-rich gases from shallow crustal magma chambers causes pre-eruptive oxidation of the reduced basalt supplied from depth. Applying either hypothesis to Kilauea leads to the expectation that the episode 1 Type II volcanic gases, which were derived from evolved basalts that experienced prolonged storage in the crust (GARCIA and WOLFE, 1988), would be relatively more oxidized than the Type I gases released in sustained summit lava lake eruptions after relatively short periods of crustal storage. The results presented in this study do not support this expectation. The Type I volcanic gases and the episode 1 Type II gases have indistinguishable oxygen fugacities. Perhaps this means that the proposed degassing processes complete the oxidation of the basalt during mantle ascent. The proposed mechanism for CO degassing, however, can only operate in the crust and is not viable at mantle pressures (MATHEZ, 1984). Therefore, if CO degassing causes the oxidation of relatively reduced basalt supplied from the mantle to Kilauea, it must do so in an essentially instantaneous manner upon arrival of the magma in the summit chamber, so that Type I and Type II gases will have the same $f_{O_2}$. The same time constraint applies for the $H_2$ diffusion mechanism if it is assumed to operate exclusively in the crust, but not if it is assumed to accomplish the required oxidation during ascent through the mantle. In either case, however, the low bulk water content of primary Kilauea tholeiitic melt (0.35 wt%), based on studies of picritic glasses thought to represent the mantle magma supplied to Kilauea (CLAGUE et al., 1991), implies an extremely low $H_2O$ activity, which may render $H_2$ diffusion ineffective as an oxidation mechanism (CARMICHAEL, 1991).

## CONCLUSIONS

Kilauea basalt either arrives in the crust with an oxygen fugacity between NNO and FMQ, or it develops an oxygen fugacity in this range immediately upon arrival in the summit chamber. The oxygen fugacities of volcanic gases emitted by subaerial lavas imply that the oxygen fugacity of Kilauea basalt changes very little during subsequent crustal storage. Volcanic gas data indicate a consistent log $f_{O_2}$ near NNO − 0.5 for subaerially erupted Kilauea basalt from liquidus to solidus temperatures.

This study challenges the common assumption that volcanic gases are released from lava in a state of chemical equilibrium and then continue equilibrating homogeneously with falling temperature until reaction rates are unable to keep pace with cooling. It also challenges the assumption that volcanic gases once released, maintain multicomponent heterogeneous equilibrium with coexisting lavas during cooling by exchanging several volatile constituents. The volcanic gases from Kilauea Volcano equilibrate with lava during cooling primarily by $f_{O_2}$ buffering through gas/lava oxygen exchange that probably involves heterogeneous ferrous/ferric redox reactions. The transfer of oxygen from $H_2O$, $CO_2$, and $SO_2$ in the gas phase to the lavas also controls the fugacities of several minor and trace gas species in addition to $O_2$. Gas/lava exchanges of other volatile components (e.g., C, H, S, Cl, F) during cooling are minor (probably negligible) and have little or no influence on gas phase equilibria. Thus, the equilibrium in Kilauea gases is a heterogeneous equilibrium constrained mainly by oxygen exchange with coexisting lavas. The equilibrium temperatures implied by the compositions of the gases reflect the temperatures at which gas/lava equilibration by oxygen exchange ceased. Higher equilibrium temperatures for the gases imply higher gas flow rates and thus shorter times for gas/lava oxygen exchange; lower equilibrium temperatures imply lower flow rates and more time for oxygen exchange reactions. Kilauea gases show no evidence that certain species are kinetically more responsive and able to equilibrate homogeneously down to lower temperatures than those of the last gas/lava oxygen exchange.

*Acknowledgments*—I am indebted to many people who helped me at various stages of this study. I thank Paul Greenland for directing me to Vent B, and the staff of the Hawaiian Volcano Observatory for logistical support. I am especially grateful to Ed Graeber for assistance in the field and to Ray Merrill, Frank Burns, Phil Rodacy, and Jim Krumhansl for assistance with the chemical analysis of the samples. Ken Ludwig provided software and consultation for the regression analysis. I thank Ian Carmichael, Mark Ghiorso, Rosalind Helz, Moto Sato, and Johan Varekamp for thoughtful review comments, and Carl Thornber and Paul Wallace for stimulating discussions. Ian Carmichael's suggestion of an appendix for details about the collection, analysis, and interpretation of the episode 1 gases helped greatly in improving an earlier version of the paper. The final responsibility for the content of the paper lies, of course, with the author. Funding for this work was provided by the USGS Volcano Hazards Program, the USGS Global Change and Climate History Program, and the US Department of Energy under contract DE-AC04-76DO00789.

*Editorial handling:* M. S. Ghiorso

## REFERENCES

ANDERSON A. T. and WRIGHT T. L. (1972) Phenocrysts and glass inclusions and their bearing on oxidation and mixing of basaltic magmas, Kilauea Volcano, Hawaii. *Amer. Mineral.* **57**, 188–216.

BALLHAUS C., BERRY R. F., and GREEN D. H. (1990) Oxygen fugacity controls in the earth's upper mantle. *Nature* **348,** 437–440.

CARMICHAEL I. S. E. (1991) The redox states of basic and silicic magmas: A reflection of their source regions?. *Contrib. Mineral. Petrol.* **106,** 129–141.

CARMICHAEL I. S. E. and GHIORSO M. S. (1986) Oxidation-reduction relations in basic magma: A case for homogeneous equilibria. *Earth Planet. Sci. Lett.* **78,** 200–210.

CARROLL M. R. and RUTHERFORD M. J. (1988) Sulfur speciation in hydrous experimental glasses of varying oxidation state: Results from measured wavelength shifts of sulfur X-rays. *Amer. Mineral.* **73,** 845–849.

CHASE M. W., JR., DAVIS C. A., DOWNEY J. R., JR., FRURIP D. J., MCDONALD R. A., and SYVERUD A. N. (1985) *JANAF Thermochemical Tables, 3rd Ed.* ACS/AIP for the NBS.

CLAGUE D. A., WEBER W. S., and DIXON J. E. (1991) Picritic glasses from Hawaii. *Nature* **353,** 553–556.

DZURISIN D., KOYANAGI R. Y., and ENGLISH T. T. (1984) Magma supply and storage at Kilauea Volcano, Hawaii, 1956–1983. *J. Volcanol. Geotherm. Res.* **21,** 177–206.

ELLIS A. J. (1957) Chemical equilibrium in magmatic gases. *Amer. J. Sci.* **255,** 416–431.

ELLSWORTH W. L. and KOYANAGI R. Y. (1977) Three-dimensional crust and mantle structure of Kilauea Volcano, Hawaii. *J. Geophys. Res.* **82,** 5379–5394.

FISKE R. S. and KINOSHITA W. T. (1969) Inflation of Kilauea Volcano prior to its 1967–1968 Eruption. *Science* **165,** 341–349.

FUDALI R. F. (1965) Oxygen fugacities of basaltic and andesitic magmas. *Geochim. Cosmochim. Acta* **29,** 1063–1075.

GARCIA M. O. and WOLFE E. W. (1988) The Puu Oo eruption of Kilauea Volcano, Hawaii: Episodes 1 through 20, January 3, 1983, through June 8, 1984—Petrology of the erupted lava. *USGS Prof. Paper* **1463,** 127–144.

GERLACH T. M. (1980) Evaluation of volcanic gas analyses from Kilauea Volcano. *J. Volcanol. Geotherm. Res.* **7,** 295–317.

GERLACH T. M. (1986) Exsolution of $H_2O$, $CO_2$, and S during eruptive episodes at Kilauea Volcano, Hawaii. *J. Geophys. Res.* **91,** 12,177–12,185.

GERLACH T. M. and GRAEBER E. J. (1985) Volatile budget of Kilauea Volcano. *Nature* **313,** 273–277.

GERLACH T. M. and NORDLIE B. E. (1975a) The C-O-H-S gaseous system, Part II: Temperature, atomic composition, and molecular equilibria in volcanic gases. *Amer. J. Sci.* **275,** 377–394.

GERLACH T. M. and NORDLIE B. E. (1975b) The C-O-H-S gaseous system, part III: Magmatic gases compatible with oxides and sulfides in basaltic magmas. *Amer. J. Sci.* **275,** 395–410.

GIGGENBACH W. F. (1975) A simple method for the collection and analysis of volcanic gas samples. *Bull. Volcanol.* **39,** 132–145.

GIGGENBACH W. F. (1987) Redox processes governing the chemistry of fumarolic gas discharges from White Island, New Zealand. *Appl. Geochem.* **2,** 143–161.

GIGGENBACH W. F. and MATSUO S. (1991) Evaluation of results from second and third IAVCEI field workshops on volcanic gases, Mt. Usu, Japan, and White Island, New Zealand. *Appl. Geochem.* **6,** 125–141.

GREENLAND L. P. (1984) Gas composition of the January 1983 eruption of Kilauea Volcano, Hawaii. *Geochim. Cosmochim. Acta* **48,** 193–195.

GREENLAND L. P. (1987) Hawaiian eruptive gases. *USGS Prof. Paper* **1350,** 759–770.

GREENLAND L. P. (1988) Gases from the 1983–84 east-rift eruption. *USGS Prof. Paper* **1463,** 145–153.

GREENLAND L. P., ROSE W. I., and STOKES J. B. (1985) An estimate of gas emissions and magmatic gas content from Kilauea Volcano. *Geochim. Cosmochim. Acta* **49,** 125–129.

HEALD E. F., NAUGHTON J. J., and BARNES I. L. (1963) The chemistry of volcanic gases. II. Use of equilibrium calculations in the interpretations of volcanic gas samples. *J. Geophys. Res.* **68,** 545–557.

HELZ R. T. and THORNBER C. R. (1987) Geothermometry of Kilauea Iki lava lake, Hawaii. *Bull. Volcanol.* **49,** 651–668.

HUEBNER J. S. and SATO M. (1970) The oxygen fugacity-temperature relationships of manganese oxide and nickel oxide buffers. *Amer. Mineral.* **55,** 934–952.

KATSURA T. and NAGASHIMA S. (1974) Solubility of sulfur in some magmas at 1 atmosphere. *Geochim. Cosmochim. Acta* **38,** 517–531.

KRESS V. C. and CARMICHAEL I. S. E. (1991) The compressibility of silicate liquids containing $Fe_2O_3$ and the effect of composition, temperature, oxygen fugacity and pressure on their redox states. *Contrib. Mineral. Petrol.* **108,** 82–92.

LUDWIG K. R. (1980) Calculation of uncertainties of U-Pb isotope data. *Earth Planet. Sci. Lett.* **46,** 212–220.

LUDWIG K. R. (1990) Isoplot: A plotting and regression program for radiogenic-isotope data, for IBM-PC compatible computers. *USGS Open-File Rep.* **88-557,** 1–31.

MACDONALD G. A. and ABBOTT A. T. (1970) *Volcanoes in the Sea, The Geology of Hawaii.* Univ. Press Hawaii.

MATHEZ E. A. (1984) Influence of degassing on oxidation states of basaltic magmas. *Nature* **310,** 371–375.

MATSUO S. (1961) On the chemical nature of fumarolic gases of Volcano Showashinzan, Hokkaido, Japan. *J. Earth Sci. Nagoya Univ.* **9,** 80–100.

MATTIOLI G. S., BAKER M. B., RUTTER M. J., and STOLPER E. M. (1989) Upper mantle oxygen fugacity and its relationship to metasomatism. *J. Geol.* **97,** 521–536.

NEAL C. A., DUGGAN T. J., WOLFE E. W., and BRANDT E. L. (1988) The Puu Oo eruption of Kilauea Volcano, Hawaii: Episodes 1 through 20, January 3, 1983, through June 8, 1984—Lava samples, temperatures, and compositions. *USGS Prof. Paper* **1463,** 99–126.

NORDLIE B. E. (1971) The composition of the magmatic gas of Kilauea and its behavior in the near surface environment. *Amer. J. Sci.* **271,** 417–463.

O'NEILL H. S. C. (1987) Quartz-fayalite-iron and quartz-fayalite-magnetite equilibria and the free energy of formation of fayalite ($Fe_2SiO_4$) and magnetite ($Fe_3O_4$). *Amer. Mineral.* **72,** 67–75.

RANDICH E. and GERLACH T. M. (1981) The calculation and use of chemical vapor deposition phase diagrams with applications to the Ti-B-Cl-H system between 1200 and 800 K. *Thin Solid Films* **75,** 271–291.

RYAN M. P., KOYANAGI R. Y., and FISKE R. S. (1981) Modeling the three-dimensional structure of macroscopic magma transport systems: Application to Kilauea Volcano, Hawaii. *J. Geophys. Res.* **86,** 7111–7129.

SAKAI H., CASADEVALL T. J., and MOORE J. G. (1982) Chemistry and isotope ratios of sulfur in basalts and volcanic gases at Kilauea Volcano, Hawaii. *Geochim. Cosmochim. Acta* **46,** 729–738.

SATO M. (1978) Oxygen fugacity of basaltic magmas and the role of gas-forming elements. *Geophys. Res. Lett.* **5,** 447–449.

SATO M. and MOORE J. G. (1973) Oxygen and sulfur fugacities of magmatic gases directly measured in active vents of Mount Etna. *Phil. Trans. Roy. Soc. London* **A274,** 137–146.

SATO M. and WRIGHT T. L. (1966) Oxygen fugacities directly measured in magmatic gases. *Science* **153,** 1103–1105.

SMITH W. R. and MISSEN R. W. (1982) *Chemical Reaction Equilibrium Analysis: Theory and Algorithms.* J. Wiley & Sons.

SPENCER K. J. and LINDSLEY D. H. (1981) A solution model for coexisting iron-titanium oxides. *Amer. Mineral.* **68,** 586–594.

STOLPER E. (1982) The speciation of water in silicate melts. *Geochim. Cosmochim. Acta* **46,** 2609–2620.

SWANSON D. A., DUFFIELD W. A., and FISKE R. S. (1976) Displacement of the south flank of Kilauea Volcano: The result of forceful intrusion of magma into the rift zones. *USGS Prof. Paper* **963,** 1–39.

THOMPSON R. N. and TILLEY C. E. (1969) Melting and crystallization relations of Kilauean basalts of Hawaii: The lavas of the 1959–60 Kilauea eruption. *Earth Planet. Sci. Lett.* **5,** 469–477.

WALLACE P. and CARMICHAEL I. S. E. (1992) Sulfur in basaltic magmas. *Geochim. Cosmochim. Acta* **56,** 1863–1874.

WOLFE E. W. (1988) The Puu Oo eruption of Kilauea Volcano, Hawaii: Episodes 1 through 20, January 3, 1983, through June 8, 1984. *USGS Prof. Paper* **1463,** 1–251.

WRIGHT T. L. and FISKE R. S. (1971) Origin of the differentiated and hybrid lavas of Kilauea Volcano, Hawaii. *J. Petrol.* **12,** 1–65.

WRIGHT T. L. and OKAMURA R. T. (1977) Cooling and crystallization of tholeiitic basalt, 1965 Makaopuhi Lava Lake, Hawaii. *USGS Prof. Paper* **1004,** 1–78.

WRIGHT T. L. and WEIBLEN P. A. (1968) Mineral composition and

paragenesis in tholeiitic basalt from Makaopuhi Lava Lake, Hawaii. *GSA Spec. Paper* **115**, 242–243.

YORK D. (1969) Least squares fitting of a straight line with correlated errors. *Earth Planet. Sci. Lett.* **5**, 320–324.

## APPENDIX

## Collection and Analysis of the Episode 1 Volcanic Gases

### *Sample collection*

The collection procedures for the Episode 1 gases were based on the widely used NaOH evacuated bottle technique (GIGGENBACH, 1975). Samples were collected in pre-weighed, evacuated 300-mL bottles filled with approximately 150 g of 4 N NaOH and sealed with a high-vacuum, O-ring type Teflon plug valve. On 14 and 15 January, a 2.5-m titanium tube (2.5 cm ID) was used to lead gases from inside the fissure to the sample bottles; a 1-m mullite tube (2.5 cm ID) was used on 16 January. The insertion depths for the "lead-in tubes" were 1.8 m on 14 January, 2.1 m on 15 January, and about 1 m on 16 January. A 20-min soak period prior to sampling permitted thermal equilibration with the gas stream and produced a protective oxide coating on the inside of the tube that minimized chemical alteration of the gas by reaction with titanium. Vigorous gas flow through the lead-in tubes produced a low whistle that was audible at distances less than about 1–2 m from the top end of the tubes. Temperatures were measured before and after collection each day. They fluctuated at these times, and probably during collection as well. Average temperatures at the base of the lead-in tubes on 14, 15, and 16 January were 935, 915, and 895°C, respectively. The top end of the tubes, where the gases were sampled with the evacuated bottles, extended 0.7 m and 0.4 m above ground level on 14 and 15 January, respectively, and had temperatures that varied from 600–700°C. The temperatures at ground level inside the lead-in tubes were approximately 775°C.

To sample the gases, an inverted, funnel-shaped metal cap was placed over the top of the lead-in tube to inhibit air contamination, and a 30 cm length of silica glass tubing was inserted through the small hole in the apex of the cap and down into the lead-in tube. The tubing was purged thoroughly before connecting it to fittings on the evacuated collection bottle. The collection bottle was inverted so that its inlet port was oriented downwards. Opening the inlet valve on the collection bottle admitted gas that bubbled up through the NaOH solution, which absorbed the acid gases ($CO_2$, $SO_2$, $H_2S$, HCl, HF) while $H_2O$ condensed and the insoluble gases ($H_2$, CO, $N_2$, $O_2$, hydrocarbon gases, rare gases) accumulated in the headspace of the bottle. Collection continued until the bottle vacuum was nearly exhausted. The average collection time was about 7 min. Bottles warmed slightly during collection.

Working conditions at the collection site were difficult. Special clothing, gloves, and head gear were required to protect against burns during collection. Gas masks were also necessary. On the whole, the performance of the sampling equipment and procedures was satisfactory. Problems were encountered, however, especially on the first day. Sample Pele 9 was directly contaminated with air during a connector failure. Another problem, one that is common with the evacuated collection bottle technique, is the tendency for a few drops of the NaOH solution containing the dissolved portion of the sample to drain out of the bottle and run down the lead-in tube if the inlet valve is not closed before the bottle vacuum is exhausted (GIGGENBACH and MATSUO, 1991). This problem affected samples Pele 6, Pele 9, and Pele 12.

### *Chemical analysis*

After collection, the sample bottles were weighed, and their head space volumes and pressures were measured. Gas chromatography and gas mass spectrometry were used to determine the composition of the gases that are nearly insoluble in the 4 N NaOH solution ($H_2$, CO, $N_2$, $O_2$, hydrocarbon gases, rare gases) and that accumulated in the head spaces of the sample bottles. Several (in some cases, redundant) techniques were used to determine the composition of the gases dissolved in the NaOH solution ($CO_2$, $SO_2$, $H_2S$, HCl, HF): ion chromatography ($SO_4^{--}$, $S^{--}$, $Cl^-$), ion specific electrode ($F^-$), chloridometry ($Cl^-$), infrared absorption ($CO_2$), gravimetric analysis ($SO_4^{--}$), and acid volumetric titration ($CO_2$). Sulfur present as $SO_2$ was determined by subtracting sulfide sulfur (measured by ion chromatography) from total dissolved sulfur (determined by gravimetric and ion chromatographic techniques) after complete oxidation of dissolved sulfur to sulfate. Sparse elemental sulfur dust was observed on the inlet port surfaces and walls of the collection bottles. Accurate extraction and weighing of the trace amounts of condensed sulfur was considered infeasible and not attempted. Similar deposits on the upper end of the 30 cm length of silica glass tubing inserted down the lead-in tube at collection indicated that some sulfur loss as elemental sulfur occurred before the gases entered the collection bottles. The amounts of water in the samples were determined by the difference between the total weight gain of the sample bottle after collection and the cumulative weight of the other gases in the sample.

Table A1 contains the analytical results; it includes sample weights, molar abundances, and mol% concentrations of major and minor species, and molar abundances of elemental components of the collected volcanic gases. All samples are of comparable size (3.03–9.40 g), although samples affected by spilling during collection (Pele 6, Pele 9, Pele 12) have the lowest sample weights. The molar abundances of species are reported to the number of significant figures warranted by the precision of the analytical data; mol% concentrations were calculated from the molar abundances and rounded to the number of significant figures. The molar abundances of elemental C, O, H, S, Cl, and F reported in Table A1 were calculated from the molar abundances of the molecular species. The estimated analytical precision (relative to reported molar abundances) is ±3% for $CO_2$, $SO_2$, CO, $H_2S$, HCl, HF, and $N_2$; for $H_2O$, $H_2$, $O_2$, and Ar, the estimated precision is ±5%. Note that $CH_4$ and higher hydrocarbons were not detected.

### Interpretation and Restoration of the Episode 1 Gas Analyses

#### *Atmospheric contamination*

The presence of measurable free $O_2$ in the samples (Table A1) indicates atmospheric contamination. The $N_2$ and Ar also appear to be primarily from atmospheric contamination. The average $N_2/Ar$ of the samples is 71.2 (Table A1), which is less than the value of air (83.6), perhaps because of minor amounts of magmatic Ar in addition to Ar from air contamination. An alternative interpretation is that it reflects releases of $N_2$ and Ar from air-saturated water, which has a lower $N_2/Ar$ than air (ca. 38 at room temperature), in fractures and pores of heated rocks near the vent. I interpret the $O_2$, $N_2$, and Ar in the gas samples to be primarily from contamination by air and/or air-saturated porewater but do not dismiss entirely the possible presence of minor magmatic $N_2$ and Ar.

The proportion of atmospheric gases in the samples is small. In most samples, the combined amount of $N_2 + Ar + O_2$ is <0.05 mol% and less abundant than $H_2$, CO, or $H_2S$ (Table A1). Pele 9, however, contains 2.54 mol% $N_2 + Ar + O_2$ from direct air contamination during a connector failure in collection, as noted previously.

Except for Pele 9, the $N_2/O_2$ values for the samples (Table A1) are much greater than the atmospheric ratio of 3.7, reflecting the consumption of atmospheric $O_2$ by chemical reaction. To estimate the maximum amounts of $O_2$ that may have been initially present, the atmospheric equivalents of $O_2$ were calculated for each sample, assuming that all the $N_2$ found is from air. The results are presented as "$O_{2,air}$" in Table A1. Only Pele 9 gives enough $O_{2,air}$ to oxidize significant amounts of $H_2$, CO, and $H_2S$; however, the mol% concentrations of these species in Pele 9 are about the same as in the other samples, indicating that significant oxidation did not occur. For the other 9 samples, $O_{2,air}$ is 1–2 orders of magnitude less than that required to oxidize all the observed $H_2$ or $H_2S$; thus, the reaction of $O_{2,air}$ with these samples would have altered $H_2$ and $H_2S$ by only noise level amounts. $O_{2,air}$ is about an order of magnitude too low to oxidize all the CO in these samples as well, except for Pele 5, which shows no evidence of CO oxidation. Even if it is assumed that all the $N_2$ found is from air and air-saturated water ($N_2/O_2 \simeq 2$) in the proportions necessary to give the average $N_2/Ar$ of the samples (71.2), the values calculated for $O_{2,air}$ only increase by about one-third—not enough to change the conclusions reached above.

The above considerations indicate that little or no oxidation of

Table A1. Sample weights, molar abundances and mole percent concentrations of major and minor species and elemental components for volcanic gases collected during episode-1 of the east rift zone eruption, Kilauea Volcano, January 1983

| Sample | Pele 9 | Pele 4 | Pele 6 | Pele 12 | Pele 2 | Pele 3 | Pele 5 | Pele 7 | Pele 8 | Pele 10 |
|---|---|---|---|---|---|---|---|---|---|---|
| Date | Jan 14 | Jan 14 | Jan 14 | Jan 15 | Jan 15 | Jan 15 | Jan 15 | Jan 15 | Jan 16 | Jan 16 |
| Collection T (°C) | 935 | 935 | 935 | 915 | 915 | 915 | 915 | 915 | 895 | 895 |
| Sample Weight (g) | 3.03 | 7.53 | 4.59 | 6.43 | 7.63 | 8.35 | 7.06 | 8.91 | 7.52 | 9.40 |
| $H_2O$ (molx$10^4$) | 701. | 2510. | 949. | 1820. | 2380. | 2720. | 2390. | 2830. | 2140. | 3050. |
| $H_2$ (molx$10^4$) | 13.59 | 30.54 | 28.33 | 33.55 | 28.10 | 28.42 | 27.14 | 32.70 | 24.32 | 27.42 |
| $CO_2$ (molx$10^4$) | 47.5 | 117. | 94.8 | 99.8 | 118. | 127. | 103. | 124. | 94.1 | 99.8 |
| CO (molx$10^4$) | 0.892 | 2.16 | 2.15 | 1.84 | 1.80 | 2.08 | 1.88 | 2.76 | 1.65 | 1.65 |
| $SO_2$ (molx$10^4$) | 224. | 370. | 367. | 363. | 407. | 420. | 342. | 493. | 483. | 519. |
| $H_2S$ (molx$10^4$) | 9.36 | 23.4 | 23.4 | 101. | 51.5 | 44.6 | 17. | 18. | 34.3 | 30. |
| HCl (molx$10^4$) | 2. | 5.27 | 4.09 | 5.27 | 4.48 | 5.47 | 4.37 | 6.12 | 4.74 | 5.78 |
| HF (molx$10^4$) | 2.8 | 6.3 | 3.3 | 6.3 | 5.8 | 5.8 | 4.2 | 6.8 | 5.1 | 5.8 |
| $N_2$ (molx$10^4$) | 23.24 | 0.391 | 0.830 | 0.741 | 0.797 | 0.578 | 4.670 | 0.684 | 0.946 | 0.8103 |
| Ar (molx$10^4$) | 0.30 | 0.0073 | 0.014 | 0.0061 | 0.027 | 0.0068 | 0.063 | 0.011 | 0.014 | 0.0099 |
| $O_2$ (molx$10^4$) | 2.6 | 0.0093 | 0.0081 | 0.016 | 0.034 | 0.015 | 0.014 | 0.011 | 0.012 | 0.014 |
| C (molx$10^4$) | 48.392 | 119.16 | 96.95 | 101.64 | 119.8 | 129.08 | 104.88 | 126.76 | 95.75 | 101.45 |
| O (molx$10^4$) | 1250.092 | 3486.1786 | 1874.7662 | 2747.472 | 3431.868 | 3816.110 | 3281.908 | 4066.782 | 3295.874 | 4289.278 |
| H (molx$10^4$) | 1452.7 | 5139.45 | 2008.85 | 3920.67 | 4929.48 | 5597.31 | 4876.85 | 5774.32 | 4407.08 | 6226.42 |
| S (molx$10^4$) | 233.36 | 393.4 | 390.4 | 464. | 458.5 | 464.6 | 359. | 511. | 517.3 | 549.0 |
| Cl (molx$10^4$) | 2. | 5.27 | 4.09 | 5.27 | 4.48 | 5.47 | 4.37 | 6.12 | 4.74 | 5.78 |
| F (molx$10^4$) | 2.8 | 6.3 | 3.3 | 6.3 | 5.8 | 5.8 | 4.2 | 6.8 | 5.1 | 5.8 |
| $H_2O$ (mol %) | 68.2 | 81.9 | 64.4 | 74.85 | 79.4 | 81.1 | 82.6 | 80.5 | 76.8 | 81.5 |
| $H_2$ (mol %) | 1.323 | 0.9964 | 1.923 | 1.380 | 0.9374 | 0.8474 | 0.9377 | 0.9305 | 0.8723 | 0.7331 |
| $CO_2$ (mol %) | 4.62 | 3.82 | 6.44 | 4.10 | 3.94 | 3.79 | 3.56 | 3.53 | 3.37 | 2.67 |
| CO (mol %) | 0.0868 | 0.0705 | 0.146 | 0.0757 | 0.0600 | 0.0620 | 0.0650 | 0.0785 | 0.0592 | 0.0441 |
| $SO_2$ (mol %) | 21.8 | 12.1 | 24.9 | 14.9 | 13.6 | 12.5 | 11.8 | 14.0 | 17.3 | 13.9 |
| $H_2S$ (mol %) | 0.911 | 0.763 | 1.59 | 4.15 | 1.72 | 1.33 | 0.59 | 0.51 | 1.23 | 0.80 |
| HCl (mol %) | 0.2 | 0.172 | 0.278 | 0.217 | 0.149 | 0.163 | 0.151 | 0.174 | 0.170 | 0.155 |
| HF (mol %) | 0.27 | 0.21 | 0.22 | 0.26 | 0.19 | 0.17 | 0.15 | 0.19 | 0.18 | 0.155 |
| $N_2$ (mol %) | 2.262 | 0.0128 | 0.0564 | 0.0305 | 0.0266 | 0.0172 | 0.1613 | 0.0195 | 0.0339 | 0.02166 |
| Ar (mol %) | 0.029 | 0.00024 | 0.00095 | 0.00025 | 0.00090 | 0.00020 | 0.0022 | 0.00031 | 0.00050 | 0.00026 |
| $O_2$ (mol %) | 0.25 | 0.00030 | 0.00055 | 0.00066 | 0.0011 | 0.00045 | 0.00048 | 0.00031 | 0.00043 | 0.00037 |
| $N_2/Ar$ (mol ratio) | 77.5 | 53.6 | 59.3 | 121. | 29.5 | 85.0 | 74.1 | 62.2 | 67.6 | 81.8 |
| $N_2/O_2$ (mol ratio) | 8.94 | 42.0 | 102.4 | 46.3 | 23.4 | 38.5 | 334. | 62.2 | 78.8 | 57.9 |
| $O_{2,air}$ (molx$10^4$)[a] | 6.23 | 0.104 | 0.223 | 0.199 | 0.214 | 0.155 | 1.25 | 0.183 | 0.254 | 0.217 |

[a] $O_{2,air} = N_2/3.728$ is the estimated maximum atmospheric $O_2$, assuming all $N_2$ is from air.

$H_2$, CO, or $H_2S$ occurred by reaction with atmospheric oxygen in these samples. It is also unlikely that significant $O_2$ reaction occurred with the titanium lead-in tube used on 14 and 15 January; the mol% concentrations of $O_2$ in samples collected on these days are similar to those of samples collected with the mullite lead-in tube on 16 January. I suggest that much of the atmospheric component present in these samples (except for Pele 9) originated by convective circulation of air or vaporized air-saturated porewater in the ground adjacent to the collection site, and that $O_2$ was lost by reaction with FeO within the surfaces of pores and fractures in cooling lavas and heated host rocks prior to entrainment by the magmatic gases feeding vent B. Consequently, atmospheric contamination in most of the samples may have occurred before and independently of collection but without disturbing significantly the redox state of the magmatic gases.

*Reactions with lead-in tubes*

The titanium lead-in tube used during collection on 14 and 15 January is potentially reactive with the high-temperature volcanic gases. The most serious concern is the reduction of the gas by the Ti. The log $f_{O_2}$ values for the Ti-$TiO_2$ buffer range from −36 to −25 between 800 and 1150°C. These log $f_{O_2}$ values are 15–25 orders of magnitude lower than those of the gas samples (Fig. 4a). It is also apparent that the $H_2$, CO, and $H_2S$ concentrations in the 14 and 15 January samples are not substantially different from the 16 January samples collected with a mullite lead-in tube. The slightly higher concentrations of $H_2$, CO, and $H_2S$ in samples Pele 9, Pele 6, and Pele 12 are shown in the discussion below to arise from spilling during collection. The HCl and HF concentrations of samples collected with the titanium lead-in tube are also similar to those of the samples obtained with the mullite tube. Thus, there is no evidence of significant chemical alteration of the samples by reactions with the titanium lead-in tube. The 20-min "soak-time" was apparently sufficient to form a reacted surface on the inside of the titanium lead-in tube that was compatible with the gases. GREENLAND (1988) reports that only 1–2 min of flushing is adequate for titanium collection tubes for Kilauea volcanic gases, but he found evidence of increased $H_2$, presumably from reduction of $H_2O$, at temperatures above 1000°C. GIGGENBACH (1975) reports titanium tubing showed chemical and mechanical stability up to 700°C in fumaroles at White Island emitting gases with HCl concentrations an order of magnitude greater than those investigated in this study.

*Testing the equilibrium hypothesis*

A primary working hypothesis for this study is that chemical equilibrium prevails in volcanic gases. This hypothesis has been employed

widely in volcanic gas research ever since ELLIS (1957) pointed out the agreement between observed volcanic gas compositions and calculated equilibrium compositions. To test the equilibrium hypothesis for the episode 1 samples, the element abundance data were used to calculate equilibrium species distributions at successively lower temperatures from 1200–800°C at 1 bar total pressure. A free energy minimization algorithm (SMITH and MISSEN, 1982) similar to those used in past studies of volcanic gases (HEALD et al., 1963; NORDLIE, 1971; GERLACH and NORDLIE, 1975a; GERLACH, 1980) provided the numerical method for computing the equilibrium distributions. All thermochemical data for the calculations are from the 1985 JANAF tables (CHASE et al., 1985). The calculations employed the Redlich-Kwong equation to approximate nonideal gas effects; however, these effects are insignificant at the high temperatures and low pressures of interest in this study. The molar abundances of C, O, H, S, Cl, and F (Table A1) defined the mass balance constraints for the calculations. The calculated species distributions for each sample consist of the equilibrium molar abundances of $H_2O$, $H_2$, $CO_2$, CO, $SO_2$, $H_2S$, HCl, and HF obtained at each temperature; these quantities are directly comparable with the analytically determined molar abundances of these species reported in Table A1.

$N_2$, Ar, and $O_2$ were neglected in the calculations since these species are interpreted to result largely from atmospheric contamination. The mass balance constraints for elemental oxygen in the equilibrium calculations were obtained by subtracting the contributions of analytically determined free $O_2$ from the molar abundances of elemental oxygen reported as "O" in Table A1; for example, the mass balance constraint for elemental oxygen in the equilibrium calculations for Pele 8 is given by the following:

$$3295.874 \times 10^{-4} \text{ mol} - 2(0.012 \times 10^{-4} \text{ mol}) = 3295.850 \times 10^{-4} \text{ mol}.$$

The neglect of any magmatic $N_2$ and Ar that may be present in the samples has little effect on the calculated species distributions because (1) the quantities are apparently very small; (2) Ar is inert; and (3) $N_2$ does not react significantly with the other gases at temperatures above 600°C, pressures near 1 bar, and at the oxygen fugacities of the episode 1 gases, which are greater than those of the fayalite-magnetite-quartz (FMQ) buffer. For example, $N_2$ and $H_2$ are stable at these conditions and do not react to form $NH_3$. Thus, $N_2$ can be considered an unreactive gas having only a negligible effect on equilibria (ELLIS, 1957).

The molar abundance obtained for a species at each temperature in the calculated equilibrium distributions for a sample is compared with its analytically determined molar abundance in Table A1. The temperature at which the calculated molar abundance of a species equals its measured molar abundance is called the "correspondence temperature" of the species (NORDLIE, 1971). For example, the correspondence temperature of CO in Pele 8 is 978°C; that is, the calculated CO molar abundance at 978°C in the 1-bar equilibrium species distribution, constrained by the element mass balances for C, O, H, S, Cl, and F given in Table A1 for Pele 8, equals the measured CO molar abundance of $1.65 \times 10^{-4}$ mol. NORDLIE (1971) introduced correspondence temperatures as a technique that permits the use of calculated equilibrium species distributions to test for equilibrium in analyses of volcanic gas samples. If the analytical compositions approach chemical equilibrium, the correspondence temperatures of all species will agree (within the limits implied by analytical precision). If the analyses are not equilibrium compositions, the correspondence temperatures will diverge by significant amounts. This approach is exactly analogous to the conventional approach of testing for equilibrium by using analytical data to calculate equilibrium constants for various reactions and examining the values obtained to determine if the temperatures they imply are in agreement (MATSUO, 1961). The reaction equilibria that are examined in the conventional approach are restricted to those involving species for which analytical data are available. Likewise, the equilibrium species distributions that are examined in the correspondence temperature approach are restricted to those species for which analytical data are available.

Table A2 contains the correspondence temperatures of $H_2O$, $H_2$, $CO_2$, CO, $SO_2$, and $H_2S$ for the ten samples. Investigations of the effects of analytical precision on correspondence temperatures indicate that equilibrium samples will have correspondence temperatures that diverge by less than ±10°C. On this basis, there are six samples that are equilibrium compositions (Pele 4, Pele 2, Pele 3, Pele 5, Pele 7, Pele 8) and four that are disequilibrium compositions (Pele 9, Pele 6, Pele 12, Pele 10). No correspondence temperatures are given for HCl and HF; their calculated molar abundances equal their measured molar abundances at all temperatures, since there are no analytical data for other Cl- and F-containing species that could react with HCl and HF. To a first approximation, HCl and HF behave like unreactive gases diluting major and minor species but have only a secondary effect on equilibria (ELLIS, 1957).

### *Causes of disequilibrium*

The disequilibrium gas samples tend to have anomalous elemental compositions, as illustrated by their molar H/C (Table A2). The equilibrium samples have H/C values between 41.15 and 46.50; however, the ratios for the disequilibrium samples are either lower (20.72–38.57) or higher (61.37) than this range. It is shown below that the divergent correspondence temperatures and anomalous H/C of the disequilibrium samples are due to excess water in Pele 10 and deficiency of water in Pele 9, Pele 6, and Pele 12.

For reasons already discussed, reactions of the gas samples with atmospheric oxygen or with the titanium lead-in tube used on 14 and 15 January are dismissed as important causes of disequilibrium. It is not likely, moreover, that these processes could alter the H/C of the gases. Perhaps certain gas species are kinetically more responsive and able to equilibrate down to lower temperatures than other species, but this would not cause variations in H/C values either. Thus, the quenching of reaction equilibria for various groups of species at different temperatures during cooling (NORDLIE, 1971; GIGGENBACH, 1987) is also dismissed as a significant cause of the observed disequilibrium. Another possible cause of disequilibrium is the partial conversion of CO to formate ion by reaction with the sodium hydroxide solution. This reaction can cause low analytical determinations for CO in collections of geothermal steam samples, but it is apparently not a serious problem in the collection of highly acid volcanic gases of the sort obtained in this study (GIGGENBACH, 1987). Furthermore, the conversion of CO to formate ion would not be capable of causing significant changes in the sample H/C, and it is unclear why just a few samples would be affected by this alteration.

The pattern in Pele 10 of high-correspondence temperatures for $CO_2$ and CO compared to lower correspondence temperatures for $H_2O$, $H_2$, $SO_2$, and $H_2S$ (Table A2) coupled with a relatively high H/C was found previously in Kilauea gases altered by contamination with water (GERLACH, 1980). While contamination by meteoric water is the most likely cause of the results for Pele 10, the divergence of the correspondence temperatures is small, however, suggesting the amount of contaminating water is minor.

In the equilibrium calculations, the excess $H_2O$ in the Pele 10 analysis in effect reacts with CO to produce $H_2$ and $CO_2$. Consequently, the amounts of $H_2O$ and CO in the equilibrium distributions

Table A2. Correspondence temperatures of major and minor species

| Sample | $H_2O$ | $H_2$ | $CO_2$ | CO | $SO_2$ | $H_2S$ | Divergence (±°C) | H/C (mol) |
|---|---|---|---|---|---|---|---|---|
| Pele 9 | 1122[a] | 1112 | 997 | 997 | 1095 | 1095 | ±62[b] | 30.02 |
| Pele 4 | 1003 | 1003 | 991 | 991 | 1001 | 1001 | ±6 | 43.13 |
| Pele 6 | 1194 | 1170 | 999 | 999 | 1139 | 1139 | ±36 | 20.72 |
| Pele 12 | 984 | 984 | 929 | 929 | 980 | 980 | ±25 | 38.57 |
| Pele 2 | 956 | 956 | 940 | 940 | 955 | 955 | ±8 | 41.15 |
| Pele 3 | 947 | 947 | 957 | 957 | 947 | 947 | ±5 | 43.36 |
| Pele 5 | 1005 | 1005 | 1000 | 1000 | 1005 | 1005 | ±2 | 46.50 |
| Pele 7 | 1025 | 1025 | 1040 | 1040 | 1025 | 1025 | ±7 | 45.55 |
| Pele 8 | 980 | 980 | 978 | 978 | 980 | 980 | ±1 | 46.03 |
| Pele 10 | 958 | 958 | 984 | 984 | 958 | 958 | ±13 | 61.37 |

[a]Correspondence temperatures in °C

[b]Range of sample correspondence temperatures in ±°C

tend to be less than their analytical amounts, while the equilibrium $H_2$ and $CO_2$ tend to exceed their analytical values. Since $H_2O$ is increasingly stable relative to $H_2$ as temperature falls, the calculated amounts of $H_2O$ and $H_2$ can only be made to agree with observed amounts at lower temperatures, which leads to the comparatively lower correspondence temperatures for these species. Since CO is increasingly stable relative to $CO_2$ at higher temperatures, the calculated and observed amounts of CO and $CO_2$ agree at higher temperatures, which leads to their higher correspondence temperatures. In like manner, the excess water also reacts with $H_2S$ in the calculations to produce $H_2$ and $SO_2$. Consequently, the amounts of $H_2O$ and $H_2S$ in the equilibrium distributions tend to be less than their analytical values, while the equilibrium $H_2$ and $SO_2$ tend to exceed their analytical values. The increasing stability of $H_2O$ relative to $H_2$ with falling temperature again leads to the comparatively lower correspondence temperatures for these species. Since $H_2S$ is increasingly stable relative to $SO_2$ at lower temperatures, the calculated and observed amounts of $H_2S$ and $SO_2$ also agree only at lower temperatures, which leads to their lower correspondence temperatures. Thus, excess water in Pele 10 causes comparatively higher correspondence temperatures for $CO_2$ and CO, and lower correspondence temperatures for $H_2O$, $H_2$, $SO_2$, and $H_2S$; of course, it also increases H/C. For purposes of illustration, Table A3 summarizes a hypothetical example (GERLACH, 1980) of the effects of disequilibrium excess water on the correspondence temperatures for a gas composition based on a composite of the Type I volcanic gases in Table 1.

Loss of water causes the opposite effects: lower H/C values; and lower correspondence temperatures for $CO_2$ and CO compared to $H_2O$, $H_2$, $SO_2$, and $H_2S$. This is the cause of disequilibrium in samples Pele 9, Pele 6, and Pele 12. Recall that spilling affected these samples during collection. Spills do not affect the analytical data for the insoluble species that accumulate in the head space of the sample bottles ($H_2$, CO). Neither do they affect significantly the data for species that dissolve in the approximately 150 g of NaOH solution ($CO_2$, $SO_2$, $H_2S$, HCl, HF), provided the spills are limited to a few drops, as was the case for these samples. Since water is determined by the difference between the weight gain of the sample bottle and the sum of the analytically determined weights of the other gas species, however, even minor spilling can cause an appreciable underdetermination of the water content of a sample, thus giving rise to low H/C values and low correspondence temperatures for $CO_2$ and CO compared to $H_2O$, $H_2$, $SO_2$, and $H_2S$.

*$H_2O$ corrections*

It is reasonable to conclude from the foregoing that the episode 1 volcanic gases were initially in a state approaching chemical equilibrium. The disequilibrium characteristics of samples Pele 9, Pele 6, and Pele 12 are due mainly to loss of water resulting from spilling. Excess water, from contamination by meteoric water caused disequilibrium in Pele 10. Therefore, it should be possible to restore the original equilibrium compositions of the four disturbed samples by subtracting water from the analysis for Pele 10 and by adding water to analyses for samples Pele 9, Pele 6, and Pele 12. Table A3 illustrates the restoration by this approach of a hypothetical gas contaminated with water.

The water contents of the disequilibrium samples were adjusted in incremental steps. At each step, the retrieval procedure calculated new elemental mass balances for O and H, new species distributions, and the resulting new correspondence temperatures. In all cases, a water content was found after a few steps that resulted in the convergence of all correspondence temperatures, indicating the original equilibrium temperatures and compositions of these samples. These results further confirm the hypothesis that the gases were initially in a state of chemical equilibrium and that the disequilibrium characteristics of these four samples are due mainly to alterations of water contents. The excess water indicated for Pele 10 is 0.77 g. The indicated water losses by spilling for Pele 9, Pele 6, and Pele 12 are 0.90, 2.14, and 1.19 g, respectively; the respective corresponding losses of dissolved gases are 0.6, 1.4, and 0.8% of the determined molar abundances presented in Table A1. The inferred equilibrium temperatures and the corrected molar abundances of $H_2O$ for the four samples are given in Table 2; no corrections were made for the losses of dissolved gases by spilling, all of which are within analytical precision.

Table A3. Effects of excess water on correspondence temperatures

| | (1) | (2) | (3) | (4) |
|---|---|---|---|---|
| $H_2O$ | 53.39[a] | 62.92 | 1013 | 53.31 |
| $H_2$ | 0.73 | 0.58 | 1018 | 0.73 |
| $CO_2$ | 33.28 | 26.47 | 1261 | 33.35 |
| CO | 1.07 | 0.85 | 1277 | 1.07 |
| $SO_2$ | 11.31 | 8.99 | 1134 | 11.32 |
| $H_2S$ | 0.05 | 0.04 | 1123 | 0.05 |

[a] mol % concentrations

(1) Calculated 1175°C equilibrium composition of a gas with H/C = 3.2 based on composite of Type I gases (Table 1).

(2) Composition of a gas obtained by adding enough excess water to (1) to give a mixture with H/C = 4.7. It is assumed that the initial gas (1) and the contaminating water do not equilibrate by reaction. (2) is analogous to an analysis of a disequilibrium volcanic gas containing excess water.

(3) Correspondence temperatures in °C for (2); i.e., temperatures at which the calculated equilibrium concentration of a species is equivalent to its concentration in (2).

(4) Restored analysis for (2) by removal of water until all correspondence temperatures agree to within ± 10 °C, as described in text. Note close agreement with (1).

*$S_2$ and COS corrections*

Up to this point, the calculated equilibrium species distributions have been restricted to those species for which analytical data are available. Numerous additional species would be present in minor amounts at equilibrium, most notably $S_2$ and COS. $S_2$ is of particular interest because of the observed loss of elemental sulfur by precipitation. It is also possible that gaseous $S_2$ and COS would dissolve in 4 N NaOH, perhaps as follows (M. Sato, pers. commun., Oct. 1991):

$$3S_2 + 6OH^- = 2SO_3^{--} + 4S^{--} + 6H^+, \quad \text{and} \qquad (A1)$$

$$COS + 2OH^- = S^{--} + CO_3^{--} + 2H^+. \qquad (A2)$$

The concentration of COS in Kilauea gases is so small (GERLACH and NORDLIE, 1975a) that its effects on analytical results for $H_2S$ ($S^{--}$) and $CO_2$ ($CO_3^{--}$) can be ignored. $S_2$ is the main elemental sulfur species in volcanic gases from basalts at the collection temperatures encountered in this study, and its concentration can be similar to that of $H_2S$ (GERLACH and NORDLIE, 1975a). If $S_2$ dissolved entirely as indicated by reaction A1, it could cause $H_2S$ to be significantly overdetermined. $SO_2$, being determined by total sulfur minus sulfide, could thus be underdetermined, but by an amount that probably would be insignificant given its high concentration in the gas samples. Since $H_2S$ has a lower molecular weight than $SO_2$, the overdetermination of $H_2S$ and underdetermination of $SO_2$ would cause a slight overdetermination of $H_2O$, but by an amount insignificant compared to the analytical precision for $H_2O$. The fact that the six equilibrium samples do not show the effects of significant $H_2S$, $SO_2$, or $H_2O$ disequilibrium (i.e., correspondence temperatures diverge by less than ±10°C) and that the four disequilibrium samples can be restored by $H_2O$ adjustments alone without altering the $H_2S/SO_2$ of the analyses suggests that $S_2$ dissolution by reaction A1 did not occur

to a significant degree. Moreover, any effects from reaction A1 on the analytical results for $H_2S$ may have been minimized by the precipitation in the bottles of solid elemental sulfur, which is relatively insoluble in NaOH compared to gaseous $S_2$, and especially by the precipitation of sulfur occurring before the gases entered the bottles, as noted above. Precipitation of sulfur in the gas stream prior to entering sample bottles is a common problem during collection of volcanic gases and has been discussed extensively over many years (MATSUO, 1961; GIGGENBACH and MATSUO, 1991). Thus, the corrections below for $S_2$ assume that the analytical data presented in Table A1 are more affected by sulfur vapor loss from precipitation of native sulfur than by $S_2$ dissolution in NaOH solution.

Coexisting amounts of $S_2$ and COS in the episode 1 gases were estimated from the following equilibria involving species that are constrained by analytical data:

$$2H_2 + SO_2 = 2H_2O + 0.5S_2, \quad \text{and} \qquad (A3)$$

$$3CO + SO_2 = COS + 2CO_2. \qquad (A4)$$

These equilibria lead to the following expressions for the equilibrium molar abundances of $S_2$ and COS in the gas samples:

$$n_{S_2} = \left[\frac{(n_{H_2})^2 n_{SO_2} K_3}{(n_{H_2O})^2 N^{1/2}}\right]^2, \quad \text{and} \qquad (A5)$$

$$n_{COS} = \frac{(n_{CO})^3 n_{SO_2} K_4}{(n_{CO_2})^2 N}, \qquad (A6)$$

where $n_i$ is the molar abundance of species $i$, $N$ is the total molar abundance of all species, and $K_3$ and $K_4$ are the 1-bar equilibrium constants for equilibria A3 and A4, respectively. The equilibrium constants were evaluated at the equilibrium temperature inferred for each sample (Table 2). For the equilibrium samples, the equilibrium temperature is taken to be the intermediate temperature between the maximum and minimum correspondence temperatures (Table A2); for the disequilibrium samples, the equilibrium temperature is the temperature obtained in the water restoration calculations described above. $N$ was first approximated by summing the molar abundances of all species (using the restored water contents for Pele 9, Pele 6, Pele 12, and Pele 10) and substituted into equilibria A5 to estimate $n_{S_2}$. Next, the estimated $n_{S_2}$ was used to obtain an improved approximation of $N$, which in turn gave a better estimate $n_{S_2}$. This process was repeated until the results for $n_{S_2}$ and $N$ converged on stable values. A similar iteration procedure was used to calculate $n_{COS}$ from equilibria A6. The resulting estimates of the molar abundances of $S_2$ and COS in each sample are presented in Table 2. From the estimates for $S_2$, sulfur losses on the order of 0.03–0.38 g by elemental sulfur precipitation are indicated, much of it perhaps prior to entering the collection bottles. The same procedures can be used to estimate compatible equilibrium amounts of other minor or trace species that may be of interest.

The mass of species neglected in the analytical determinations contributes to the reported amount of $H_2O$ because water is determined by the difference between the weight gain of the sample bottle and the sum of the analytically determined weights of the other gas species. This introduces an excess water error in the data reported for $H_2O$. The error is small, however, because the quantities of neglected species are small. In the cases of the samples showing disequilibrium due to water loss by spilling, the amounts of water lost are vastly greater than the excess water due to neglected species; thus, spilling nullified any excess water due to neglected species. In Pele 10, which showed disequilibrium from excess water, the correction made to restore the water content also accounted for any excess water due to neglected species. For the equilibrium samples, the amount of excess water implied by the neglected species is insignificant relative to the analytical precision for $H_2O$. For example, the amount of excess $H_2O$ ($n_{ex,H_2O}$) implied by the molar abundances of $S_2$ (assuming the worst case where all $S_2$ is precipitated as elemental sulfur after entering the collection bottle) can be calculated from the following:

$$n_{ex,H_2O} = n_{2_2}(64\ \text{g/mol})/(18\ \text{g/mol}) = 3.556 n_{S_2}. \qquad (A7)$$

The value for $n_{ex,H_2O}$ is always within the analytical precision for $H_2O$ in the equilibrium samples. This result is consistent with the fact that the divergence of the correspondence temperatures (±°C; Table A2) shows no correlation with the estimated mol% $S_2$ concentrations in the equilibrium samples (Fig. A1).

*Restored analyses*

The restored gas compositions are summarized in Table 2. Table 2 contains the same molar abundances as Table A1 for species that are unchanged by the corrections made above. The molar abundances of $H_2O$ in Table 2 are the same as those in Table A1 for the equilibrium samples; however, the corrected molar abundances for $H_2O$ are reported for those samples with altered water contents. Table 2 includes the estimated equilibrium molar abundances of $S_2$ and COS in all samples. The molar abundances of the elemental components C, O, H, and S in Table 2 have been recalculated for the $H_2O$ corrections and the inclusion of $S_2$, and COS. The mol% concentrations given in Table 2 are based on the restored molar abundances. Included in Table 2 are the log values for the fugacities of $O_2$, $Cl_2$, and $F_2$ (in bars) calculated from the restored compositions at the inferred equilibrium temperatures.

**Comparison with Other Episode 1 Gas Data**

GREENLAND (1984) reported the analyses for three episode 1 gas samples collected in the vicinity of Vent B on 17 and 18 January with the same mullite tube that was used in this study. Temperatures at the base of the mullite tube on these dates were between 863 and 887°C. The analyses for the three samples are reproduced in Table A4 along with correspondence temperatures that were calculated in the course of the present study. The analyses are similar to those presented here except for their somewhat higher $H_2O$ contents.

The correspondence temperatures are moderately divergent and indicate disequilibrium. The pattern is the same in all three cases: low values for $H_2O$, $H_2$, $SO_2$, and $H_2S$ relative to $CO_2$ and CO. This pattern indicates excess water, as in Pele 10, and this interpretation is supported by the higher H/C (54–71.5) of the analyses compared to the equilibrium samples reported in this study. The data reported by GREENLAND (1984) and in this study indicate relatively uniform gas compositions for the episode 1 gases. When the analyses of GREENLAND (1984) are plotted on a C-H-S ternary diagram (Fig. A2) along with the restored analyses from Table 2, their somewhat higher water contents are evident, but the overall agreement of the two data sets is good.

GREENLAND (1987) also published numerous estimated compositions for episode 1 gases based on calculations from partial analyses of "continuous flow" samples. Continuous flow samples are collected by pumping fumarole gases through a glass bottle with stopcock valves at both ends. The stopcock valves are shut to trap a gas sample in

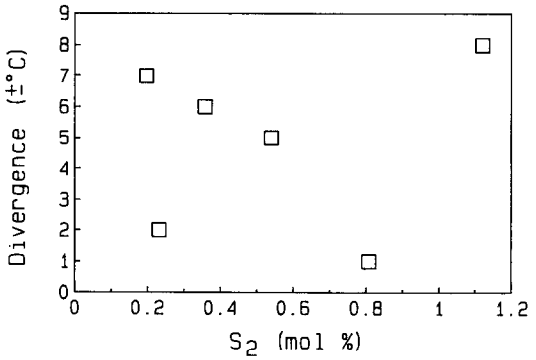


FIG. A1. Divergence of correspondence temperatures (±°C, Table A2) for equilibrium samples vs. their estimated mol% $S_2$ concentrations (Table 2). Divergence is uncorrelated with mol% $S_2$ for these samples.

the bottle after several seconds of pumping. The samples are analyzed within a few hours by gas chromatography for only $CO_2$, CO, $SO_2$, $H_2$, $N_2$, and $O_2$ + Ar; a complete analysis is normally not attempted for continuous flow gas samples. GREENLAND (1987) used the data from the partial analyses of episode 1 continuous flow samples to estimate equilibrium temperatures and $O_2$ fugacities and coexisting equilibrium amounts of $H_2O$ and $H_2S$, thus obtaining an estimated complete gas composition. This method for estimating complete gas compositions depends crucially on the assumption that an equilibrium gas was sampled and on the acquisition of gas chromatography data before significant oxidation of $H_2$ and $SO_2$ by reactions with contaminating atmospheric $O_2$ in the sample bottle, which tends to be enhanced in continuous flow samples due to pumping during collection. $SO_2$ is lost by oxidation to $SO_3$, which dissolves readily in the condensate formed in the sample bottle and goes undetected by gas chromatography.

The estimated episode 1 gas compositions obtained by GREENLAND (1987) from thirty-four continuous flow samples collected at temperatures above the local boiling point are plotted in Fig. A2. Figure A2 includes the restored gas compositions (Table 2) and the complete analyses from Table A4 for comparison. A least-squares linear regression curve based on all the data in Fig. A2 projects to the H apex of the ternary diagram and indicates that the variations in the data are related primarily to differences in water contents. Most of the estimated compositions are depleted in water relative to the restored gas samples of Table 2. The most water-rich estimated compositions, however, do converge with the restored gas compositions of this study. Since the $H_2O$ content calculated for the estimated gas compositions is directly proportional to the square of the $H_2$ concentration, oxidation of $H_2$ is the most likely cause of the low water contents obtained for most of the estimated compositions.

Table A4. Episode 1 gas compositions from Greenland (1984)

| | Jan 17 | Jan 18(#1) | Jan 18(#2) |
|---|---|---|---|
| $H_2O$ | 85.2[a] ( 973)[b] | 84.8 ( 948) | 82.9 (1000) |
| $H_2$ | 0.85 ( 973) | 0.62 ( 948) | 0.86 (1000) |
| $CO_2$ | 3.16 (1022) | 2.33 (1140) | 2.94 (1080) |
| CO | 0.068(1022) | 0.078(1140) | 0.084(1080) |
| $SO_2$ | 9.58 ( 978) | 11.3 ( 960) | 12.3 (1005) |
| $H_2S$ | 0.53 ( 978) | 0.39 ( 960) | 0.49 (1005) |
| HCl | 0.32 | 0.21 | 0.20 |
| HF | 0.26 | 0.26 | 0.26 |
| | (±24)[c] | (±96) | (±40) |

[a]mol % concentrations

[b]Correspondence temperatures (°C)

[c]Range of sample correspondence temperatures in ±°C

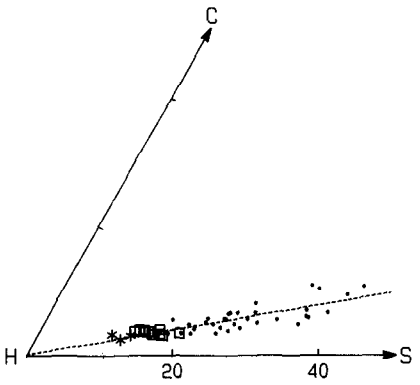


FIG. A2. Ternary plot of restored gas compositions (squares) from Table 2, complete analyses of GREENLAND (1984) for episode 1 gases (asterisks) from Table A4, and calculated gas compositions of GREENLAND (1987) from partial analyses of continuous flow samples from episode 1 (small circles). The dashed line is the least-squares linear regression curve for all the data. The regression curve extrapolates to the H apex and is consistent with the interpretation that variations in the data are mainly related to differences in the water content of the gas compositions. The ternary components are in mol% units defined as in Fig. 3.

The continuous flow sampling technique (or so-called "flow through" sampling technique) is used commonly during eruptions because it offers quick analytical results, and it has proven reliable for monitoring the C/S ratio of gases during eruptions at Kilauea (GREENLAND, 1984). It is recommended on the basis of the present study, however, that gas chromatography analyses of continuous flow samples not be used to calculate the complete composition of volcanic gases from basalts, unless rough estimates are acceptable. This sampling procedure is prone to atmospheric contamination with the consequence that $H_2$ oxidation causes the estimation scheme to give low water contents for the gas.

I conclude that the restored compositions presented in Table 2 represent the best available estimate of the composition of the magmatic component in the gases emitted during episode 1 of the Puu Oo eruption. It is possible, however, that even these compositions may contain minor contamination introduced at temperatures above the last equilibrium temperatures of 935–1032°C (Table 2) inferred in the above analysis of the data.